

# STUDIES ON OPTIMIZATION OF LAMINATED COMPOSITE PLATES

SHIV PRAKASH JUMBI



# STUDIES ON OPTIMIZATION OF LAMINATED COMPOSITE PLATES

A Thesis Submitted  
in Partial Fulfilment of the Requirements  
for the Degree of  
MASTER OF TECHNOLOGY

By  
SHIV PRASAD JOSHI

in the  
DEPARTMENT OF AERONAUTICAL ENGINEERING  
INDIAN INSTITUTE OF TECHNOLOGY, KANPUR

## 04-0115-72

This is to certify that the work STUDIES ON OPERATIONAL  
ON ENHANCED COMPOSITE P-32 has been carried out  
under my supervision and has not been submitted elsewhere  
for a degree.

*N.G.R. 3-4-7*  
(M.A. 10118)  
Professor  
Department of Aero. Engg.  
I.I.T. Bombay

POST OFFICE BOX 1000  
 EL PASO TEXAS 79901  
 (915) 782-1000  
 (915) 782-1001  
 (915) 782-1002  
 (915) 782-1003  
 (915) 782-1004  
 (915) 782-1005  
 (915) 782-1006  
 (915) 782-1007  
 (915) 782-1008  
 (915) 782-1009  
 (915) 782-1010  
 (915) 782-1011  
 (915) 782-1012  
 (915) 782-1013  
 (915) 782-1014  
 (915) 782-1015  
 (915) 782-1016  
 (915) 782-1017  
 (915) 782-1018  
 (915) 782-1019  
 (915) 782-1020  
 (915) 782-1021  
 (915) 782-1022  
 (915) 782-1023  
 (915) 782-1024  
 (915) 782-1025  
 (915) 782-1026  
 (915) 782-1027  
 (915) 782-1028  
 (915) 782-1029  
 (915) 782-1030  
 (915) 782-1031  
 (915) 782-1032  
 (915) 782-1033  
 (915) 782-1034  
 (915) 782-1035  
 (915) 782-1036  
 (915) 782-1037  
 (915) 782-1038  
 (915) 782-1039  
 (915) 782-1040  
 (915) 782-1041  
 (915) 782-1042  
 (915) 782-1043  
 (915) 782-1044  
 (915) 782-1045  
 (915) 782-1046  
 (915) 782-1047  
 (915) 782-1048  
 (915) 782-1049  
 (915) 782-1050  
 (915) 782-1051  
 (915) 782-1052  
 (915) 782-1053  
 (915) 782-1054  
 (915) 782-1055  
 (915) 782-1056  
 (915) 782-1057  
 (915) 782-1058  
 (915) 782-1059  
 (915) 782-1060  
 (915) 782-1061  
 (915) 782-1062  
 (915) 782-1063  
 (915) 782-1064  
 (915) 782-1065  
 (915) 782-1066  
 (915) 782-1067  
 (915) 782-1068  
 (915) 782-1069  
 (915) 782-1070  
 (915) 782-1071  
 (915) 782-1072  
 (915) 782-1073  
 (915) 782-1074  
 (915) 782-1075  
 (915) 782-1076  
 (915) 782-1077  
 (915) 782-1078  
 (915) 782-1079  
 (915) 782-1080  
 (915) 782-1081  
 (915) 782-1082  
 (915) 782-1083  
 (915) 782-1084  
 (915) 782-1085  
 (915) 782-1086  
 (915) 782-1087  
 (915) 782-1088  
 (915) 782-1089  
 (915) 782-1090  
 (915) 782-1091  
 (915) 782-1092  
 (915) 782-1093  
 (915) 782-1094  
 (915) 782-1095  
 (915) 782-1096  
 (915) 782-1097  
 (915) 782-1098  
 (915) 782-1099  
 (915) 782-1100  
 (915) 782-1101  
 (915) 782-1102  
 (915) 782-1103  
 (915) 782-1104  
 (915) 782-1105  
 (915) 782-1106  
 (915) 782-1107  
 (915) 782-1108  
 (915) 782-1109  
 (915) 782-1110  
 (915) 782-1111  
 (915) 782-1112  
 (915) 782-1113  
 (915) 782-1114  
 (915) 782-1115  
 (915) 782-1116  
 (915) 782-1117  
 (915) 782-1118  
 (915) 782-1119  
 (915) 782-1120  
 (915) 782-1121  
 (915) 782-1122  
 (915) 782-1123  
 (915) 782-1124  
 (915) 782-1125  
 (915) 782-1126  
 (915) 782-1127  
 (915) 782-1128  
 (915) 782-1129  
 (915) 782-1130  
 (915) 782-1131  
 (915) 782-1132  
 (915) 782-1133  
 (915) 782-1134  
 (915) 782-1135  
 (915) 782-1136  
 (915) 782-1137  
 (915) 782-1138  
 (915) 782-1139  
 (915) 782-1140  
 (915) 782-1141  
 (915) 782-1142  
 (915) 782-1143  
 (915) 782-1144  
 (915) 782-1145  
 (915) 782-1146  
 (915) 782-1147  
 (915) 782-1148  
 (915) 782-1149  
 (915) 782-1150  
 (915) 782-1151  
 (915) 782-1152  
 (915) 782-1153  
 (915) 782-1154  
 (915) 782-1155  
 (915) 782-1156  
 (915) 782-1157  
 (915) 782-1158  
 (915) 782-1159  
 (915) 782-1160  
 (915) 782-1161  
 (915) 782-1162  
 (915) 782-1163  
 (915) 782-1164  
 (915) 782-1165  
 (915) 782-1166  
 (915) 782-1167  
 (915) 782-1168  
 (915) 782-1169  
 (915) 782-1170  
 (915) 782-1171  
 (915) 782-1172  
 (915) 782-1173  
 (915) 782-1174  
 (915) 782-1175  
 (915) 782-1176  
 (915) 782-1177  
 (915) 782-1178  
 (915) 782-1179  
 (915) 782-1180  
 (915) 782-1181  
 (915) 782-1182  
 (915) 782-1183  
 (915) 782-1184  
 (915) 782-1185  
 (915) 782-1186  
 (915) 782-1187  
 (915) 782-1188  
 (915) 782-1189  
 (915) 782-1190  
 (915) 782-1191  
 (915) 782-1192  
 (915) 782-1193  
 (915) 782-1194  
 (915) 782-1195  
 (915) 782-1196  
 (915) 782-1197  
 (915) 782-1198  
 (915) 782-1199  
 (915) 782-1200  
 (915) 782-1201  
 (915) 782-1202  
 (915) 782-1203  
 (915) 782-1204  
 (915) 782-1205  
 (915) 782-1206  
 (915) 782-1207  
 (915) 782-1208  
 (915) 782-1209  
 (915) 782-1210  
 (915) 782-1211  
 (915) 782-1212  
 (915) 782-1213  
 (915) 782-1214  
 (915) 782-1215  
 (915) 782-1216  
 (915) 782-1217  
 (915) 782-1218  
 (915) 782-1219  
 (915) 782-1220  
 (915) 782-1221  
 (915) 782-1222  
 (915) 782-1223  
 (915) 782-1224  
 (915) 782-1225

# CONTENTS

	Page
ABSTRACT	vi
LIST OF TABLES	vi
LIST OF FIGURES	viii
LIST OF SYMBOLS	x
CHAPTER 1    Review of the Literature	1
1.1 Introduction	1
1.2 Literature Survey	4
1.3 Objective and Scope of the present work	7
CHAPTER 2    OPTIMAL DESIGN OF LATERAL PLATES UNDER UNIFORM AXIAL COMPRESSION	9
2.1 Introduction	9
2.2 Optimization Procedure	10
2.3 Problem Formulation	11
2.3.1 Analysis	12
2.3.2 Restriction of Buckling Load	14
2.3.3 Constraints and their Gradients	14
2.4 Results and Discussion	17
2.4.1 Results	17
2.4.2 Explanation of Results	20
2.5 Conclusions	22

Table no.		Page
1.1	Effect of Number of Plies on Maximum Buckling Load	15
1.2	Variation of Maximum Buckling Load with Aspect Ratio	15
1.3	Variation of Maximum Buckling Load with Elastic Loading Ratio	15
1.4	Optimum Buckling Load considering Thickness and Fiber Orientation as Design Variables	19
1.5	The Optimum Values of the Ply Thickness and Corresponding Fiber Orientation for a Plate (with only unimodular loading applied)	24
1.6	Variation of Optimum Values with Aspect Ratio and Elastic Loading Ratio	29
4.1	Variation in the Optimum Weights with change in pre-assigned arbitrary Fiber Orientation	42
4.2	Variation in the Optimum Ply Thickness with Total Number of Plies	43

Chapter No.		Page
4.1	Variation in the Constant Fly Thickness with Total Number of Fibers	84
4.2	Variation in Fly Thickness with change in pre-assigned Fiber Orientation	85
4.3	Variation of Optimum Fiber Orientation and corresponding Thickness	86
4.4	Optimum Fiber Orientation and Corresponding Fly Thickness	87

Figure No.		Page	
1.1 (a)	Co-ordinate system & fiber orientation	154a)	
1.1 (b)	Stacking sequence - co-ordinate system for the layered plate.	154b)	
1.2	Variation of Buckling load with Fiber Orientation	36	
1.3	Variation of Buckling load with Fiber Orientation	37	
1.4	Change in Fiber Orientation during Optimization	38	
1.1	Maximum Deflection of simply supported Laminated Plate vs.Fiber Orientation	65	
1.2	Variation of Longitudinal Stress with Fiber Orientation	66	
1.3	Variation of Transverse Stress with Fiber Orientation	67	
1.4	Variation of Shear Stress with Fiber Orientation	68	
1.5	Variation of Optimum Weight with Aspect Ratio	69	
1.6	Variation of Deflection and Buckling Load with Aspect Ratio for Optimum Weight Design	70	

Figure No.		Page
3.3	variation of optimum height with barrel loading ratio	71
4.1	Thickness Ratio vs. Total Number of Fills	88



## LIST OF SYMBOLS

$\tau, b$	= Dimensions of the glass
$\bar{A}_{ij}, \bar{B}_{ij}, \bar{D}_{ij}$	= Global constants of the composite plate
$\bar{N}_x, \bar{N}_y$	= In-plane normal forces
$\bar{M}_x$	= Bending moment on section load per unit width
$K$	= Ratio of in-plane normal stresses ( $\bar{\sigma}_x/\bar{\sigma}_y$ )
$\bar{Q}_{ij}$	= Reduced stiffnesses at layer $i$ along $j$ fiber orientation angles
$q$	= Transverse loading
$t_i$	= Thickness of $i^{\text{th}}$ lamina
$u, v$	= In-plane displacements
$w$	= Transverse displacement
$\epsilon_x, \epsilon_y, \epsilon_{xy}$	= Strain components in the xy-plane
$\sigma_x, \sigma_y, \sigma_{xy}$	= In-plane stresses
$\theta$	= Fiber orientation of the lamina
$v_i$	= Design variables
$N^*$	= Total number of design variables
$N$	= The number of plies in laminate

STUDIES ON OPTIMIZATION OF LAMINATED COMPOSITE PLATES  
BY P. KANAKA JOSE

M. Tech. Thesis

Department of Aeronautical Engineering  
Indian Institute of Technology, Madras

ABSTRACT

Studies are carried out for the minimum weight optimum design of laminated fiber composite plates, subjected to multiple inplane loadings and transverse loadings. The behaviour constraints are on stability, strength and deflection. Angle-ply laminates with orthotropic laminae and antisymmetric angle-ply laminates are considered for optimization studies. The orthotropic property is achieved by taking an equal number of fibers at positive and negative orientations, with respect to structural axis in the former case. Thickness of plies and corresponding fiber orientations are incorporated as design variables while the number of plies is treated as a design parameter. The constrained optimization problem is transformed into a series of unconstrained optimization problems, using an interior penalty function approach. The results have been obtained for different aspect ratios and various classical boundary loading ratios. This study shows that the fiber orientations

of thickness and modulus have little effect on the optimum design. They select a particular fiber orientation angle for the overall thickness of laminate, which results in the optimum design for a plate of a given aspect ratio under a given set of loadings. In case of antisymmetric angle-ply laminates, particular ratios of ply thickness result in the optimum design of the plate. It has been observed that the number of plies have no effect on the optimum design.

## 5.1.2.1

### 5.1.2.1.1 Fiber-reinforced composites

#### 5.1.2.1.1.1 Fiber-reinforced composites

During the last two decades or so, fiber reinforced laminates have found increasing applications in many engineering structures. They are largely used in structural components for both primary and secondary structures. The fiber reinforced composites possess two valuable features, one is their high stiffness-to-weight and strength-to-weight ratio, and the other is their anisotropic strength properties, even one of anisotropy through variation of the fiber orientation. This thickness of plies and stacking sequence - , features which gives the designer an added degree of flexibility to achieve the desired strength or stiffness in any direction. The ever-increasing use of composites have stimulated interest in the development of optimal design of structures made of composite materials.

Laminated plates constitute an important structural element in aerospace, mechanical and civil engineering structures. Laminated fibrous composites are a class of composites involving both fibrous composites and laminated techniques. Here, layers of fiber reinforced material are built up with the fiber direction of each layer typically oriented in different directions, to give different strengths and stiffnesses in the various directions, as achieved by the

designed. The uses of laminated fiber reinforced composites include fuselage, wings, floor structure, nacelle cases, aircraft wing boxes and joint sections, power systems, propellers, fire-glass door panels, various structural and other applications.

In aerospace applications, where weight saving is of paramount importance, the uses of high modulus/ high-strength fiber reinforced composites materials such as carbon/fiberglass and graphite/epoxy, has resulted in a dramatic increase in the use of laminated fiber reinforced plates and other structural shapes as primary structural members. The past, present and future of the composites in aircraft and space vehicles can be summarized as follows: The advanced composites were developed around 1960 and then the conceptual and structural developments were demonstrated. Up to 1974, small components of hardware had been developed and flight tested. At present, large primary structures are being constructed. The test journals reveal that the plans to build airplanes by using up to 40 percent composite materials. The final stage is the all-composite airplanes which will be seen in the near future. To achieve this, obviously, construction techniques have been applied to get overall weight designs with desirable structural properties.

In the next section, a survey of the existing literature pertaining to development is presented.

### 3.1.2. Optimal design

Optimization in structural design has been recognized as early as 1970, [1] [2-11] and the optimum use of reinforced-concrete structures as a design criterion.

Most et al. [4] has used an efficient structural method based on strain energy minimization for optimal design for the minimum weight design of structures made from fiber reinforced composites. The opt. or min procedure takes into consideration elastic linear conditions and displacement control into the structure. As is evident consisting of two distinct and composite structures are solved and the results obtained.

Lee and Chou [5] used a direct search procedure to optimize layered structures subjected to dynamic loading conditions. The technique is a hill climbing method of search design for minimum weight design of the structures. Layered structures under time varying load and transient loads respectively.

Lehoucq and Engel [6] proposed a method for minimum weight design of composite structures subjected to multiple in-plane loading conditions which can lead to more efficient structures and

arbitrary dimensions, the problem is cast as a nonlinear mathematical programming problem in which the objective of maximization is a design variable with prescribed orientation angles.

Johnson et. al. (7) applied optimality criteria to the iterative reanalysis of the elements of finite element used to analyze various wing types. The program sequentially creates a single generalized displacement or strain, and multiple constraints can be accounted for in each case or mechanical interest by multiple maximization of program.

Johnson (8) wrote a computer program which can be used to estimate or analyze a composite structure. Response of the structure to the applied loads is obtained by finite element analysis. The design variables are modified during each iteration by using a recurrence relation. The four strength criteria included in the program are:

maximum stress, maximum strain, Hill's criterion modified by Tsai, and Morris criterion. The plate elements can be designed to permit local buckling.

Johnson (9) presented an algorithm based on the simplex method of linear programming, without linearizing the non-linear mixed integer programming problem involving the number of layers, their thickness and their fiber directions. Orthotropic layers were used and the Anisotropy of the

analysis ranging from the design of optimum shape and size of the composite. It is known that all are not available in such a range of thickness and size which always be possible.

Johnson (13,14) dealt with the problem of minimizing all layer fiber reinforced composite, i.e. a relation variables are the total deflection of the finite element model. It is shown that genetic is more use for solving the nonlinear mixed integer program involved and shows the optimal number of layers in each layer. The layer thickness and the fiber angles were determined simultaneously for very general inequality constraints on stress and deflections.

Chen et. al. (15) determined optimum orientation for a symmetric composite laminate consisting of layers of  $+45^\circ$  and  $-45^\circ$  fiber orientations and subjected to in-plane loadings. Stability of both the laminate and laminate yield are evaluated. The loading results oriented are restricted to specially orthotropic laminate while the first laminate yield is allowed to initiate laminate failure.

Schiff and Jershi (16) presented a method for the minimum weight optimum design of laminated fiber composite plates, subjected to various in-plane loading conditions.



These include stiffeners, stiffeners, and elastic buckling analysis, the buckling analysis is based on an eigenvalue problem to give an exact. This approach is appropriate for highly loaded, balanced, symmetric laminates or skins relatively large number of plies. The approach for technique used is a series of linear programming techniques with constraint deletion technique in conjunction with layerwise analysis for the constraints and not, uniformity of value and number of plies are used as design variables. This linear orientation is given in 5.

Hayashi (14) proposed optimum design of plywise ratio of angle ply laminates. The fiber orientation are selected for the corresponding buckling stress, the however, the cost, and the thickness of the laminate is to be minimized.

Simons (15) carries out the optimum design of laminated plates with orthotropic layers under uniaxial and biaxial compression. Anisotropy is achieved by using equal number of fibers with +ve and -ve orientation in the same ply. Laminate plate is made up of plies that equal thickness. Fiber orientation of each ply is selected as design variable while the number of plies is prescribed. Specific composite direction is used to maximize the buckling stress.

desirable shape of  $\theta$ ,  $\alpha$ , and  $\beta$  have been obtained. The variable  $\theta$  consists of plates, the bending effect of coupling out is illustrated, and the aim is to increase in the strength of the laminates.

The variety of the form, type, laminates on the various ranges of laminated composites which are used, and all the design variables have been calculated to arrive at an optimal design. Since fiber orientation of thickness of a ply has been the use of a design variable, there is more a systematic study of combination of composite plates is required by taking into account all the possible design variables.

### 3.1.2. THE DESIGN PROBLEM WITH COMPOSITE PLATES

The design problem with composite involves the determination of thickness distributions and corresponding fiber orientations. Thickness for each fiber orientation can change is subdivided into layers which of plates with given fiber orientation. It may now be necessary because of manufacturing limitations. The priority will be slight variation in thickness in order to get integer number for plates can be exploited, which are the design variables and the design variables thickness or composition of the number of plates to be an integer. The thickness distribution and corresponding fiber orientation should be chosen.



A study of the buckling under biaxial compression is presented in Chapter 2. Buckling load is maximized to understand the behavior of fiber orientations. The second problem in chapter 2 incorporates thickness of each ply in addition to the fiber orientation as design variables.

Chapter 3 deals with an optimum weight design of composite plate under in-plane and transverse loadings. Composite plate created with orthotropic laminae is considered. Each lamina's principal directions coincide with structural axes.

Anisotropic angle-ply laminates are considered in chapter 4, for optimization studies with constraints on stress, deflection and buckling load.

Chapter 5 summarizes the results of the investigation. A short note is added to indicate the extension of the present work.

# On the Theory of the Elasticity of the

of the Elasticity of the

## 1. Introduction

Since the early 19th century the theory of elasticity has become a well-developed branch of applied mathematics. It has been applied to a wide range of problems, from the design of structures to the study of the behavior of materials under stress. The theory is based on the assumption that the material is homogeneous and isotropic, and that the deformation is small. The basic equations of the theory are the equilibrium equations, the constitutive equations, and the compatibility equations. The equilibrium equations are derived from the principle of conservation of momentum, and the constitutive equations are derived from the assumption of a linear relationship between stress and strain. The compatibility equations are derived from the requirement that the displacement field must be continuous. The theory of elasticity has been applied to a wide range of problems, from the design of structures to the study of the behavior of materials under stress. The basic equations of the theory are the equilibrium equations, the constitutive equations, and the compatibility equations. The equilibrium equations are derived from the principle of conservation of momentum, and the constitutive equations are derived from the assumption of a linear relationship between stress and strain. The compatibility equations are derived from the requirement that the displacement field must be continuous.

The present study is devoted to the study of the behavior of the theory of elasticity with varying thickness of the plates and membranes. The theory is based on the assumption that the material is homogeneous and isotropic, and that the deformation is small. The basic equations of the theory are the equilibrium equations, the constitutive equations, and the compatibility equations. The equilibrium equations are derived from the principle of conservation of momentum, and the constitutive equations are derived from the assumption of a linear relationship between stress and strain. The compatibility equations are derived from the requirement that the displacement field must be continuous. The theory of elasticity has been applied to a wide range of problems, from the design of structures to the study of the behavior of materials under stress. The basic equations of the theory are the equilibrium equations, the constitutive equations, and the compatibility equations. The equilibrium equations are derived from the principle of conservation of momentum, and the constitutive equations are derived from the assumption of a linear relationship between stress and strain. The compatibility equations are derived from the requirement that the displacement field must be continuous.

The study is carried out for the following:

- (I) Determination of a layered composite plate for maximum bearing load with constraint on each ply to be within a prescribed thickness.
- (II) Optimization of a layered composite plate for average bearing load with constraint on the total thickness of laminate to be within a prescribed value.

### 2.2. Mathematical Formulation

In constrained optimization problem considered in Sec. 2.1, to find a vector of design variables  $\mathbf{v}$  that minimizes the bearing load  $f(\mathbf{v})$  of a plate subject to the constraints

$$G_i(\mathbf{v}) \leq 0 \quad i = 1, m \quad (1)$$

It is assumed that at least one of the constraints of

Eq. (1) is active at the optimal point, that is,  $G_1(\mathbf{v}) = 0$  for some  $i$ . This constrained minimization problem may be transformed into a series of unconstrained minimization problems by introducing a Lagrangian function  $L(\mathbf{v}, \lambda)$  which is defined as follows. In the case where  $m$  constraints are active at the optimal point,  $L(\mathbf{v}, \lambda)$  is defined as follows and on the other hand

$$L(\mathbf{v}, \lambda) = f(\mathbf{v}) + \lambda \sum_{i=1}^m G_i(\mathbf{v}) \quad (2)$$



### 2.2.1. Equations

Fig. 1.1 (a) shows an arbitrary ply (see 1.1) curved at  $\pm\theta$  to  $\pm\psi$  fiber orientations. It should be noted that  $\bar{\sigma}_{yy}$  and  $\bar{\tau}_{xy}$  are identically zero.

The three governing equations along  $x, y$  and  $z$  are (15)

$$\begin{aligned} \sigma_{11} - \sigma_{33} - \sigma_{22} \epsilon_{yy} + (\epsilon_{12} + \epsilon_{22}) \sigma_{xy} - \epsilon_{11} \sigma_{xx} \\ - (\epsilon_{12} + 2\epsilon_{22}) \sigma_{xy} = 0 \end{aligned} \quad (15)$$

$$\begin{aligned} (\epsilon_{12} + \epsilon_{22}) \sigma_{xy} + \sigma_{22} \sigma_{xx} + \sigma_{21} \sigma_{yy} = (\epsilon_{12} + 2\epsilon_{22}) \\ \sigma_{xy} - \sigma_{21} \sigma_{yyy} = 0 \end{aligned} \quad (16)$$

$$\begin{aligned} -\sigma_{11} \sigma_{xxx} + 2(\epsilon_{12} + 2\epsilon_{22}) \sigma_{xyy} - \sigma_{21} \sigma_{yyy} \\ - \epsilon_{11} \sigma_{xxx} - (\epsilon_{12} + 2\epsilon_{22}) \sigma_{xy} - \epsilon_{12} + 2\epsilon_{22} \sigma_{xy} \\ - \sigma_{22} \sigma_{yyy} + \sigma_x \sigma_{xx} - \sigma_y \sigma_{yy} = 0 \end{aligned} \quad (17)$$

where (see Fig. 1.1(b))

$$\begin{aligned} \epsilon_{1j} &= \frac{h}{k+1} (\bar{\epsilon}_{1j})_k \quad (\epsilon_x = \epsilon_{k+1}) \\ \epsilon_{2j} &= \frac{1}{h} \frac{d}{dz} (\bar{\epsilon}_{1j})_k \quad (\epsilon_y^2 = \epsilon_{k+1}^2) \\ \epsilon_{3j} &= 1/\sqrt{2} \frac{d}{dz} (\bar{\epsilon}_{1j})_k \quad (\epsilon_y^3 = \epsilon_{k+1}^3) \end{aligned} \quad (18)$$

and

$$\sigma_y = \sigma \quad \sigma_x = \sigma$$



split the result in two parts, and can  
 be used to represent conditions, for example the  
 analysis is restricted to supply supported boundary  
 conditions, which are used for optimization studies.  
 When  $x, y$ , and  $z$  in the following, need to satisfy simply  
 supported boundary conditions,

$$x = \bar{x} \cos (n \pi y/a) \sin (m \pi z/a) \quad (1)$$

$$y = \bar{y} \sin (n \pi x/a) \cos (m \pi z/a) \quad (2)$$

$$z = \bar{z} \sin (n \pi x/a) \sin (m \pi y/a)$$

Substituting these assumed functions (1) in the governing  
 equations (3,4,5) , and further simplification gives us as

$$A_{nm} = \frac{2}{a^2} \frac{1}{a^2} \left[ \frac{1}{a^2} + \frac{1}{a^2} \left( \frac{a}{b} \right)^2 \right] \left[ A_{11} + \frac{2}{a_{11} a_{12} - a_{12}^2} \frac{a_{11}^2 - a_{12}^2}{a_{11} a_{12} - a_{12}^2} \right] \quad (10)$$

where

$$a_{11} = a_{11}^0 \pi^2 + a_{11}^0 \pi^2 \left( \frac{a}{b} \right)^2$$

$$a_{12} = a_{12}^0 + a_{12}^0 \pi^2 \left( \frac{a}{b} \right)$$

$$a_{13} = a_{13}^0 \pi^2 + (a_{13}^0 + 2 a_{12}^0) \pi^2 \left( \frac{a}{b} \right)^2$$

$$a_{22} = a_{22}^0 \pi^2 + a_{22}^0 \pi^2 \left( \frac{a}{b} \right)^2$$

$$\begin{aligned}
 \sigma_{22} &= \sigma_{12} + \sigma_{22} \gamma^2 \pi^2 (a/b)^2 + \sigma_{22} \gamma^2 \pi^2 (a/b)^2 \\
 \sigma_{22} &= \sigma_{12} \gamma^2 \pi^2 + 2 ( \sigma_{12} + 2 \sigma_{22} ) \pi^2 \gamma^2 (a/b)^2 \\
 &\quad + \sigma_{22} \gamma^4 \pi^4 (a/b)^4
 \end{aligned}$$

### 2.1.3. Derivatives of the objective function

The  $\gamma$ -discorder of optimization algorithms requires the gradient of objective function and constraints. Derivative computation leads to two function evaluation at each design point which leads to higher computational time. Because of the complex nature of the function, truncation errors increase and hence produce erroneous which produces/decreases the efficiency of the algorithm. Derivatives of critical axial load with respect to design variables, which include thickness of ply and corresponding orientations, are obtained as follows.

Let  $\tau_i$  be design variable  $i = 1, 2$

For this case,

$$\tau_1 = t_k \quad i = 1, \quad \tau_2 = \theta_k \quad i = 2, \quad k = 1, 2, \dots, 16$$

Differentiation of Eq. (20) gives,

$$\begin{aligned}
 \frac{\partial \sigma_{22}}{\partial \tau_1} &= \frac{2}{\pi^2 a^2 \{ \pi^2 + 2 \pi^2 (a/b)^2 \}} \left[ \frac{\partial \sigma_{22}}{\partial \tau_1} \right] \\
 &= \sigma_{12} \sigma_{22} = \sigma_{12} + 2 \frac{\partial \sigma_{22}}{\partial \tau_1} \sigma_{22} + 2 \frac{\partial \sigma_{22}}{\partial \tau_2} \sigma_{12} \sigma_{22}
 \end{aligned}$$

2.1.3. Derivatives of the objective function

$$\begin{aligned}
& + 2 \frac{\partial^2 \mathcal{L}_{12}}{\partial^2 \sigma_1} \sigma_{12} \sigma_{13} = \frac{\partial^2 \mathcal{L}_{22}}{\partial^2 \sigma_1} \sigma_{12}^2 + 2 \frac{\partial^2 \mathcal{L}_{12}}{\partial^2 \sigma_1} \sigma_{13} \\
& - \frac{\partial^2 \mathcal{L}_{12}}{\partial^2 \sigma_1} \sigma_{22}^2 + 2 \frac{\partial^2 \mathcal{L}_{12}}{\partial^2 \sigma_1} \sigma_{11} \sigma_{22} = (2 \sigma_{12} \sigma_{22} - \sigma_{13}^2) \\
& - \sigma_{12} \sigma_{22}^2 = \sigma_{11} \sigma_{22}^2 + \left( \frac{\partial^2 \mathcal{L}_{12}}{\partial^2 \sigma_1} \sigma_{12} + \frac{\partial^2 \mathcal{L}_{22}}{\partial^2 \sigma_1} \sigma_{12} \right. \\
& \left. + 2 \frac{\partial^2 \mathcal{L}_{12}}{\partial^2 \sigma_1} \sigma_{22} \right) / (\sigma_{12} - \sigma_{22} - \sigma_{13}^2)^2 \quad (12)
\end{aligned}$$

where,

$$\begin{aligned}
\frac{\partial^2 \mathcal{L}_{11}}{\partial^2 \sigma_1} &= \frac{\partial^2 \mathcal{L}_{11}}{\partial^2 \sigma_1} \sigma^2 \pi^2 + \frac{\partial^2 \mathcal{L}_{11}}{\partial^2 \sigma_1} \sigma^2 \pi^2 (a_r/b)^2 \\
\frac{\partial^2 \mathcal{L}_{12}}{\partial^2 \sigma_1} &= \left( \frac{\partial^2 \mathcal{L}_{12}}{\partial^2 \sigma_1} + \frac{\partial^2 \mathcal{L}_{12}}{\partial^2 \sigma_1} \right) m \pi \pi^2 (a_r/b) \\
\frac{\partial^2 \mathcal{L}_{13}}{\partial^2 \sigma_1} &= \frac{\partial^2 \mathcal{L}_{13}}{\partial^2 \sigma_1} \pi^2 \pi^2 + \left( \frac{\partial^2 \mathcal{L}_{13}}{\partial^2 \sigma_1} + 2 \frac{\partial^2 \mathcal{L}_{13}}{\partial^2 \sigma_1} \right) m \sigma^2 \pi^2 (a_r/b)^2 \\
\frac{\partial^2 \mathcal{L}_{22}}{\partial^2 \sigma_1} &= \frac{\partial^2 \mathcal{L}_{22}}{\partial^2 \sigma_1} \sigma^2 \pi^2 + \frac{\partial^2 \mathcal{L}_{22}}{\partial^2 \sigma_1} \sigma^2 \pi^2 (a_r/b)^2 \quad (13) \\
\frac{\partial^2 \mathcal{L}_{23}}{\partial^2 \sigma_1} &= \left( \frac{\partial^2 \mathcal{L}_{23}}{\partial^2 \sigma_1} + 2 \frac{\partial^2 \mathcal{L}_{23}}{\partial^2 \sigma_1} \right) m^2 \pi \pi^2 (a_r/b) \\
&+ \frac{\partial^2 \mathcal{L}_{23}}{\partial^2 \sigma_1} \sigma^2 \pi^2 (a_r/b)^2 \\
\frac{\partial^2 \mathcal{L}_{33}}{\partial^2 \sigma_1} &= \frac{\partial^2 \mathcal{L}_{33}}{\partial^2 \sigma_1} \sigma^2 \pi^4 + 2 \left( \frac{\partial^2 \mathcal{L}_{33}}{\partial^2 \sigma_1} + 2 \frac{\partial^2 \mathcal{L}_{33}}{\partial^2 \sigma_1} \right) m^2 \sigma^2 \pi^4 \\
&(a_r/b)^2 + \frac{\partial^2 \mathcal{L}_{33}}{\partial^2 \sigma_1} \sigma^4 \pi^4 (a_r/b)^4
\end{aligned}$$

Components of  $\sigma_{ij}$ ,  $\epsilon_{ij}$  and  $\beta_{ij}$  as eq. (8a) have been reflected at various angles as shown in figs. These stiffness matrices are a function of, both fiber orientation and thickness of ply. Expressions for gradients of stiffness matrices are given in Appendix I.

### 2.1.1. First problem: $\theta = 0$ , $\phi = 0$

Constraints and their derivatives for the first problem stated earlier, are as follows :

Following constraints are imposed on the first problem

$$v_1 = 1 - v_2/v_1^2 \quad i = 1, 1'/2 \quad (14)$$

$$v_2 = 1 - v_2/v_1^2 \quad i = 1'/2 + 1, 1' \quad (15)$$

and

$$v_1 - v_1' = v_2 \quad i = 1, 1' \quad (16)$$

Derivatives of equation 14, 15 and 16 are as follows

$$\frac{\partial v_1}{\partial v_j} = -\delta_{ij} \quad 1/v_1^2 \quad \text{for } i = 1, 1'/2 \quad j=1, 1' \quad (17)$$

$$\frac{\partial v_2}{\partial v_j} = -\delta_{ij} \quad 1/v_1^2 \quad \text{for } 1+1'/2 = 1, 1' \quad j=1, 1' \quad (18)$$

Following constraints are imposed on the second problem.

$$v_2 = 1 - \left( \sum_{i=1}^{1'/2} v_1 \right) / v_1^2 \quad (19)$$

$$\epsilon_2 = 1 - \frac{2k_2}{h_2} \frac{h_2}{2} \quad i = 2, h'/2 + 1 \quad (20)$$

Derivatives of constraints are

$$\frac{\partial g_j}{\partial x_j} = -\frac{k_j}{t} \quad j = 1, h'/2 \quad (21)$$

$$0 \quad j = h'/2 + 1, h'$$

$$\frac{\partial g_j}{\partial x_j} = -\frac{k_j}{h_j} \quad 1/h'/2 \quad \text{for } i = 2, h'/2 + 1$$

$$\text{where, } i + h'/2 = 1 \quad j = 1, h'$$

## 2.1. MATERIAL PROPERTIES

### 2.1.1. Kevlar

Optimization studies have been carried out on rectangular composite plates, taking into consideration number of plies, aspect ratio and biaxial loading ratio as parameters for Kevlar/Epoxy composite whose material properties are as follows:

$$E_1 = 1.1 \times 10^4 \text{ kg/cm}^2$$

$$E_2 = 1.1 \times 10^3 \text{ kg/cm}^2$$

$$\nu_{12} = 0.3$$

$$\rho_{12} = 1.3 \times 10^3 \text{ kg/cm}^3$$

Numerical computations have been carried out on ILL 1600 computer. Results obtained for two sets of constraints considered are as follows:

### 3.3.3.3)

Table 3.1 shows typical results obtained by varying number of piles. This indicates that the number of piles has no effect on maximum buckling load. Oriented plate assumes orthotropic properties as optimum design occurs, by orienting, forces of all the piles in the direction which results in maximum buckling load. However the loss, conventional results obtained, by considering higher number of piles provided some useful & sign informations which are discussed later in this section.

The variation of maximum buckling load w.r. aspect ratio is shown in Table 3.2. The optimum fiber orientation increases from  $0^\circ$  to  $90^\circ$  with increasing aspect ratio for uniaxial loading. However, <sup>for</sup> biaxial loading with  $(\sigma_y / \sigma_x) = 1.5$ , the variation in fiber orientation is approximately from  $0^\circ$  to  $45^\circ$  for a change in aspect ratio from 3.5 to 4.5.

Table 3.3 shows that the buckling load decreases with increasing biaxial loading ratio. The optimum fiber orientation remains zero for a square plate. However, for rectangular plate it increases with biaxial loading ratio. Typical results for aspect ratio 3.5 are presented in this table.

### 3.4.3.16)

Table 3.4 presents the optimum fiber orientation and corresponding buckling load for laminated parts. When total thickness is constant, the thickness of each ply can vary. These results indicate that the thickness of plies whose orientation is less than  $45^\circ$  being fixed unquestioned minimization, show up, this means, other plies should increase thickness to satisfy the condition of constant total thickness. In general, thickness of outer most plies increases, even. In cases where initial orientations of inner plies are very close to optimal, while fiber orientation of outer plies are far away.

The variation of buckling load with fiber orientation for orthotropic laminated plate is shown in Fig. 3.3. Aspect ratio of plate is 1.25 and compressive load is applied along x direction only. It is observed that for fiber orientations up to  $55^\circ$ , a half sine wave in x-direction and a half sine wave in y-direction is the primary mode of buckling, but for higher orientations primary mode of buckling is one half sine wave in x-direction and one half sine wave in y-direction. Fiber orientation of  $55^\circ$  gives maximum buckling load and the value of buckling also changes at this orientation. Fig. 3.5 presents similar analysis for aspect ratio 3.0 and  $E_y/E_x = 0.5$ .

Fig. 1.5 presents variation in fiber orientation for each unconfined  $\sigma_2$  compression direction during sequential deformation.

### 3.4.2. Buckling Load at 45°

Fiber orientation of 45° leads to maximum buckling load for a square cross section uniaxial compression (Table 1.1), that, this will be so can be verified in the following manner.

Consider Eq. (10), which is reproduced in a dimensionless form, from  $\lambda_1$ , (11) and (13) it is inferred that  $\tau_{11}$  predominantly contributes to the buckling load. For carbon is case, where  $\nu = 0$ , only  $\tau_{12}$  contributes to the buckling load:

$$P = \frac{12 \lambda_1^2 \pi^2}{\pi^2 \lambda_1^2 Q_{22}} = \frac{12 (E_2/\pi)^2}{\pi^2 \lambda_1^2 Q_{22} \left\{ \pi^2 + 2 \pi^2 (E_2/\pi)^2 \right\}} + \left[ \sigma_{11} + \frac{2 \lambda_{12} \tau_{21} \lambda_{13} - \tau_{22} \tau_{13} - \lambda_{11} \sigma_{13}^2}{\lambda_{11} \lambda_{22} - \tau_{12}^2} \right] \quad (14)$$

where

$$\begin{aligned} \tau_{11} = \pi^2 \left[ \lambda_{11} \pi^2 + 2 (D_{11} + 2 \lambda_{22}) \pi^2 \pi^2 (E_2/\pi)^2 \right. \\ \left. + \lambda_{22} \pi^2 (E_2/\pi)^2 \right] \end{aligned} \quad (15)$$

The buckling stiffness coefficient  $\lambda_{11}$  decreases with increase in orientation from 0° to 90°. At 90°,  $\lambda_{11}$  is



equal to  $\Omega_{22}$  at  $0^\circ$ ,  $\Omega_{22}$  decreases with orientation from  $0^\circ$  to  $90^\circ$ ,  $\Omega_{22}$  at  $90^\circ$  is equal to  $\Omega_{11}$  at  $0^\circ$ , to  $45^\circ$ ,  $\Omega_{11}$  and  $\Omega_{22}$  are a  $\Delta\omega$ . In case of shear deformation, we can easily verify that  $\Omega_{33}$  is maximum at fiber orientations are at  $45^\circ$  ( $n = 1$  and  $n = 1$  is the primary axis of buckling). This corroborates the results obtained by optimization study.

It may be noted that  $\Omega_{22}$  is the expression for  $\Omega_{33}$  as,  $(\sigma)$  is multiplied by  $(\sigma/\tau)^4$  and  $2(\Omega_{12} + 2\Omega_{33})$  is multiplied by  $(\sigma/\tau)^2$ . If aspect ratio  $(\sigma/\tau)$  is less than one, then contribution of  $\Omega_{22}$  diminishes with decreasing aspect ratio and  $\Omega_{11}$  tries to push optimum fiber orientation towards  $0^\circ$ ,  $2(\Omega_{12} + 2\Omega_{33})$  and  $\Omega_{22}$  try to hold it back, as a result the optimum fiber orientation is in between  $0^\circ$  and  $45^\circ$ . For aspect ratio greater than one  $\Omega_{22}$  contributes prominently and hence tries to pull up the fiber orientation. This results in the optimum fiber orientation between  $45^\circ$  and  $90^\circ$ . The above argument holds good if primary mode of buckling is a half sine wave in x and y-directions respectively. The average in buckling mode, averages contribution of each term in  $\Omega_{33}$  equation which results in decrease in fiber orientation angle from  $45^\circ$  to  $49^\circ$  for higher aspect ratios.

The means for changing its side shape (or an orthotropic laminae plate (all cases with same fiber orientations) are discussed below.

(a) with  $n = 1$ , the change in the side shape occurs, when

$$J_{12} \text{ (rad.)} = J_{12} \text{ (rad.)} \cdot \text{mod}$$

(load applied in x-direction only)

This results in

$$\begin{aligned} \frac{J_{12}}{J_{11}} \frac{D_{11}}{D_{22}} &= \alpha^2 + 2(D_{12} + D_{22}) \alpha^2 (a/b)^2 + J_{22} (a/b)^4 \cdot \\ &= \frac{1}{(n+1)^2} \alpha^2 \left[ J_{11} (n+1)^4 + 2 (J_{12} + D_{22}) (n+1)^2 (a/b)^2 \right. \\ &\quad \left. + J_{22} (a/b)^4 \right] \end{aligned} \quad (25)$$

Further simplification results in

$$(a/b)^4 = \frac{(2n+1)}{\left( \frac{J_{12}}{J_{11}} = \frac{1}{(n+1)^2} \right)} \cdot \frac{D_{11}}{D_{22}} \quad (26)$$

Eq. (26) gives the exact ratio at which side shape along x-direction changes. It is evident from equation (26) that the exact ratio at which side shape changes, depends on the material properties. For a plate of given thickness Eq. (26) can further be simplified, as,

$$(a/b)^4 = \frac{(2n+1)}{\left( \frac{J_{12}}{J_{11}} = \frac{1}{(n+1)^2} \right)} \cdot \frac{D_{11}}{D_{22}} \quad (27)$$

Let  $\bar{G}^0$  and  $\bar{G}_{22}^0$  represent the reduced stiffness coefficients at optimum fiber orientation, then

$$(a/b)^4 = \frac{(\bar{G}_{22}^0)}{r^2 - \frac{\bar{G}_{22}^0}{\bar{G}_{22}^0}} \quad (28)$$

and  $n = 1$

$$(a/b)^4 = 4 - \frac{\bar{G}_{22}^0}{\bar{G}_{22}^0} \quad (29)$$

In order to obtain the aspect ratio for change in ratio of  $x$ -direction at optimum fiber orientation, expression for optimum fiber orientation is derived. The variation for optimality with respect to fiber orientation is

$$\frac{\partial^2 \bar{G}}{\partial \theta^2} = 0 \quad i = 1, 2$$

Reducing eq. (26) to an orthotropic case and its differentiation results in

$$2 \bar{G}_{11}^0 r^4 + 2 (\bar{G}_{22}^0 + 2 \bar{G}_{22}^0) a^2 b^2 (r/b)^2 + 2 \bar{G}_{22}^0 n^4 (a/b)^4 = 0 \quad (30)$$

where  $\bar{G}_{ij}^0$  are derivatives of coupling stiffness coefficients with respect to fiber orientation, defined as below,

$$\bar{G}_{ij}^0 = 1/3 \frac{\partial^2}{\partial \theta^2} (\bar{G}_{ij}^0) = (a_k^2 - a_{k-1}^2) = \frac{a_k^2}{12} - \bar{G}_{ij}^0 \quad (31)$$

where,

$$\begin{aligned} Q_{11}^* &= 2 U_2 \sin 2\alpha + 2 U_3 \sin 4\alpha \\ Q_{12}^* &= 2 U_3 \sin 4\alpha \\ Q_{22}^* &= 2 U_2 \sin 2\alpha + 2 U_3 \sin 4\alpha \\ Q_{33}^* &= 2 U_3 \sin 4\alpha \end{aligned} \quad (4.2)$$

$U_2$  and  $U_3$  are defined as

$$\begin{aligned} U_2 &= \frac{a_{11} - a_{22}}{2} \\ U_3 &= \frac{a_{13} - a_{23} - a_{31} - a_{32}}{2} \end{aligned} \quad (4.3)$$

Substituting Eq. (4.2) in Eq. (4.1) and after simplification it yields,

$$\begin{aligned} U_2 \sin 2\alpha^* + 2 U_3 \sin 4\alpha^* (a_2/b)^4 + 2 U_3 \sin 4\alpha^* \\ (a_2/b)^2 + U_2 \sin 2\alpha^* + 2 U_3 \sin 4\alpha^* (a_2/b)^4 = 0 \end{aligned} \quad (4.4)$$

Eq. (4.4) gives the value of optimum fiber orientation for a given aspect ratio. To verify qualitative arguments given earlier, substitute  $a_2/b = 1$  in Eq. (4.4). It reduces to,

$$\sin 4\alpha^* = 0$$

and hence for maximum  $\sin 4\alpha^* = 1$  at  $\alpha^* = 1/4$  (45) (4.5)

For  $h/b = 1.25$  (Fig. 2.2) solving Eq. (41) by trial and error equations, the following is obtained:

$$\mu^* = 1.57.5 \quad \text{Eq. (42)}$$

Solving Eq. (42) for the optimum fiber orientation the aspect ratio came out to be 1.35 for a change in mode shape along x-direction (red to 2). It shows that change in mode shape occurs in summer.

(c)  $n = 1$ , proceeding in a similar way, the following equations are obtained:

$$(u_1/u_2)^2 = \frac{(2n^2 + 1)}{(4n^2 + 6n^2 + 4n + 1)} \cdot \frac{2G_{12}^2 + 2G_{22}^2}{G_{22}^2} \quad (43)$$

or,

$$(u_1/u_2)^2 = \frac{(1/2n^2 + 1)}{(4n^2 + 6n^2 + 4n + 1)} \cdot \frac{2G_{12}^2 + 2G_{22}^2}{G_{22}^2} \quad (44)$$

for  $n = 1$

$$(u_1/u_2)^2 = \frac{1}{2} \cdot \frac{2G_{12}^2 + 2G_{22}^2}{G_{22}^2} \quad (45)$$

For biaxial loading, the aspect ratio at which the mode of twisting changes, becomes a complex function of rotational stiffness and mode of fiber orientation. For  $n = 1$ ,

Eq. (45) defines a vert ratio for which mode of twisting changes from  $n$  to  $(-1)^2$  and is given below by

$$(a_1/a_2)^2 = \frac{2(1-\nu)(4m^2 + 4m^2 + 4m + 1) + 2}{1}$$

$$= \frac{2(1-\nu)(4m^2 + 4m^2 + 4m + 1) + 2(4m^2(2m^2 + 1)m^2 + 4m^2 + 4m + 1)}{1}$$

$$\frac{(2m+1)(\Omega_{22} - 2\nu\Omega_{12} + 2\nu_{22}^2)\tau_{21}}{(2m+1)\Omega_{22} - 2\nu\Omega_{12} + 2\nu_{22}^2} \tau_{21} \quad (49)$$

$$2(2m+1)\Omega_{22} - 2\nu\Omega_{12} + 2\nu_{22}^2$$

Fig. 2.3 shows that crossing of mod. 1,2 and mod. 1,1 occurs at an orientation  $\theta^* = 10^\circ$  which gives the maximum buckling load. This is plotted for an aspect ratio  $R, 1$  and  $K = 1, 3$ .

Table 2.2 reveals that fiber orientation of inner and outer plies do not contribute much to maximum buckling load. It has been shown earlier that  $\tau_{33}$  contributes predominantly to buckling load and it involves having a different consideration. If  $\bar{\tau}_{12}$  is zero for all the plies then the outermost ply contributes maximum to  $\tau_{12}$ .  $(a_2^2 = a_{2-1}^2)$  is maximum for outer ply due to which  $\tau_{33}$  is maximum, which gives the maximum buckling load. Analogous with respect to fiber orientations for case 2b same kind of results. Fig. 2.4 shows that fiber orientation of outer plies affects buckling load and fiber orientation of inner plies affects buckling load equally. The latter may contribute before reaching optimum orientation without giving much difference in maximum buckling load.

Results for design buckling load with varying thickness and fiber orientations are presented in Table 2.4. Derivatives at maximum load with respect to thickness and fiber orientation at each  $\mu_1$  are such that, the thickness of the  $\mu_1$  layer reaches optimum as total design fiber orientation varies. Proof by inspection: It is to enable a smaller fraction of the plate thickness to achieve optimum orientation. Further for this case also verify that contribution of glass thickness near mid-span is not remarkable to the other 'net' fiber orientations are important.

### 2.4. CONCLUSIONS

From the above study the following conclusions can be drawn.

- (1) Maximum buckling load is obtained when total thickness of the plate assumes the optimum fiber orientation for a given aspect ratio and blade loading ratio. However fiber orientation and corresponding thickness can be determined in such a way that they are almost equivalent to the total thickness having optimum fiber orientation.
- (2) Since the optimum is obtained when total thickness assumes an optimum orientation, approximation techniques

*Handwritten notes:*  
 1. The optimum fiber orientation is achieved when the total thickness of the plate is oriented in the same direction as the fiber orientation.  
 2. The optimum fiber orientation is achieved when the total thickness of the plate is oriented in the same direction as the fiber orientation.  
 3. The optimum fiber orientation is achieved when the total thickness of the plate is oriented in the same direction as the fiber orientation.

can be applied to a two ply plate to obtain optimum orientation. The results obtained by using an optimum design  $\theta$  plate of given aspect ratio for uniform loading by varying the total thickness of plate when and as needed with cases of given thickness with various fiber orientations.

- (13) The designer of a composite plate for maximum buckling load can work with relax manufacturing tolerance as far as plates near the mid-plane are concerned.
- (14) In general, optimal fiber orientation is such that, slight change in orientation changes primary mode of buckling; If a designer is interested in the mod. of failure, he can choose fiber orientation slightly away from the optimum to ensure particular mode without any significant change in critical buckling load. Any fiber orientation between  $40^\circ$  and  $50^\circ$  will result in almost maximum buckling load with associated mode 1:1 for a plate of aspect ratio 1.25 (Fig. 2.3). Fiber orientation between  $10^\circ$  and  $15^\circ$  will result in maximum buckling load with associated mode 1:1 for a plate of aspect ratio 1.5 and identical loading ratio 0.5 (Fig. 2.3).



Table 7.1 : 2000 to 2005 in terms of  $\beta$  on a 1000 iteration basis

Iteration	2000-2005 in terms of $\beta$	Calculated $F_{\text{max}}$ (Iteration/Iteration)						Reduced artificial pool $\beta$	code of the library
		$\beta_1$	$\beta_2$	$\beta_3$	$\beta_4$	$\beta_5$	$\beta_6$		
1	1.0	0.0	45.0	47.0				21.977	1.1
		0.0	44.9	46.0	44.0			21.977	1.1
2	1.0	0.0	45.0	46.0	45.0			21.977	1.1
		0.0	45.9	43.0	41.1			21.977	1.1
3	1.0	0.0	45.0	45.0	45.0			21.977	1.1
		0.0	44.0	45.9	45.5	45.4	46.5	21.977	1.1
4	1.0	0.0	45.0	45.0	45.0	45.0	45.1	21.977	1.1
		0.0	44.0	45.4	45.5	45.4	46.5	21.977	1.1

Book 7-7, "Sustaining the World: The World and the World's People"

[illegible]

Table 2.2 (Contd.)

Joint position	Applied load (kN)	$\Delta_1$	Column fiber orientation (deg)				Reduced vertical load P	Angle of twist (deg)
			$\Delta_2$	$\Delta_3$	$\Delta_4$	$\Delta_5$		
A	2.0	0.0	44.9	49.0	44.9	44.9	45.0	45.0
			45.0	49.0	45.0	45.0	45.0	45.0
	0.5	0.5	45.8	50.0	45.8	45.8	45.8	45.8
			45.9	50.0	45.9	45.9	45.9	45.9
	1.0	0.5	45.8	49.0	45.8	45.8	45.8	45.8
			45.9	49.0	45.9	45.9	45.9	45.9
	2.0	0.5	45.8	49.0	45.8	45.8	45.8	45.8
			45.9	49.0	45.9	45.9	45.9	45.9
	2.0	0.5	45.8	49.0	45.8	45.8	45.8	45.8
			45.9	49.0	45.9	45.9	45.9	45.9

Table 2.1. Summary of the data obtained for the various samples, as in

No. of plates	No. of plates (No. of plates)	Optimum fiber concentration						Reduced viscosity (ml/g)	Time of boiling
		wt. %	wt. %	wt. %	wt. %	wt. %	wt. %		
0	1.0	0.0	0.0	0.0	0.0	0.0	0.0	20.000	1.0
		0.5	0.5	0.5	0.5	0.5	0.5	15.00	1.0
		0.0	0.0	0.0	0.0	0.0	0.0	20.000	1.0
	4.0	0.0	0.0	0.0	0.0	0.0	0.0	20.000	1.0
		0.5	0.5	0.5	0.5	0.5	0.5	15.00	1.0
		0.0	0.0	0.0	0.0	0.0	0.0	20.000	1.0
	8.0	0.0	0.0	0.0	0.0	0.0	0.0	20.000	1.0
		0.5	0.5	0.5	0.5	0.5	0.5	15.00	1.0
		0.0	0.0	0.0	0.0	0.0	0.0	20.000	1.0
	12.0	0.0	0.0	0.0	0.0	0.0	0.0	20.000	1.0
		0.5	0.5	0.5	0.5	0.5	0.5	15.00	1.0
		0.0	0.0	0.0	0.0	0.0	0.0	20.000	1.0

Handwritten notes and signature:

Handwritten text: *Handwritten text*

Signature: *Handwritten signature*

1991, 2004, 2005) – is used to model the interaction and fitting parameters for the two types of neurons.

[!\[\]\(2e897e890e69d81eae4503a8342c36b0\_img.jpg\)](#)
[!\[\]\(ce4e2504c7100a62a9a9496b2e01b6e4\_img.jpg\)](#)
[!\[\]\(d6653e1cf2c96f17cfd897a08e4b2bd5\_img.jpg\)](#)

Case No.	$\frac{V_{max}}{V_0}$	$V_{max}$	$V_0$	$\frac{V_{max}}{V_0}$	$V_{max}$	$V_0$	Initial concentration mole/l	Final concentration mole/l
1	0.0	0.0	0.0	0.0	0.0	0.0	0.0	0.0
2	0.0	0.0	0.0	0.0	0.0	0.0	0.0	0.0
3	0.0	0.0	0.0	0.0	0.0	0.0	0.0	0.0
4	0.0	0.0	0.0	0.0	0.0	0.0	0.0	0.0
5	0.0	0.0	0.0	0.0	0.0	0.0	0.0	0.0
6	0.0	0.0	0.0	0.0	0.0	0.0	0.0	0.0
7	0.0	0.0	0.0	0.0	0.0	0.0	0.0	0.0
8	0.0	0.0	0.0	0.0	0.0	0.0	0.0	0.0
9	0.0	0.0	0.0	0.0	0.0	0.0	0.0	0.0
10	0.0	0.0	0.0	0.0	0.0	0.0	0.0	0.0
11	0.0	0.0	0.0	0.0	0.0	0.0	0.0	0.0
12	0.0	0.0	0.0	0.0	0.0	0.0	0.0	0.0
13	0.0	0.0	0.0	0.0	0.0	0.0	0.0	0.0
14	0.0	0.0	0.0	0.0	0.0	0.0	0.0	0.0
15	0.0	0.0	0.0	0.0	0.0	0.0	0.0	0.0
16	0.0	0.0	0.0	0.0	0.0	0.0	0.0	0.0
17	0.0	0.0	0.0	0.0	0.0	0.0	0.0	0.0
18	0.0	0.0	0.0	0.0	0.0	0.0	0.0	0.0
19	0.0	0.0	0.0	0.0	0.0	0.0	0.0	0.0
20	0.0	0.0	0.0	0.0	0.0	0.0	0.0	0.0
21	0.0	0.0	0.0	0.0	0.0	0.0	0.0	0.0
22	0.0	0.0	0.0	0.0	0.0	0.0	0.0	0.0
23	0.0	0.0	0.0	0.0	0.0	0.0	0.0	0.0
24	0.0	0.0	0.0	0.0	0.0	0.0	0.0	0.0
25	0.0	0.0	0.0	0.0	0.0	0.0	0.0	0.0
26	0.0	0.0	0.0	0.0	0.0	0.0	0.0	0.0
27	0.0	0.0	0.0	0.0	0.0	0.0	0.0	0.0
28	0.0	0.0	0.0	0.0	0.0	0.0	0.0	0.0
29	0.0	0.0	0.0	0.0	0.0	0.0	0.0	0.0
30	0.0	0.0	0.0	0.0	0.0	0.0	0.0	0.0
31	0.0	0.0	0.0	0.0	0.0	0.0	0.0	0.0
32	0.0	0.0	0.0	0.0	0.0	0.0	0.0	0.0
33	0.0	0.0	0.0	0.0	0.0	0.0	0.0	0.0
34	0.0	0.0	0.0	0.0	0.0	0.0	0.0	0.0
35	0.0	0.0	0.0	0.0	0.0	0.0	0.0	0.0
36	0.0	0.0	0.0	0.0	0.0	0.0	0.0	0.0
37	0.0	0.0	0.0	0.0	0.0	0.0	0.0	0.0
38	0.0	0.0	0.0	0.0	0.0	0.0	0.0	0.0
39	0.0	0.0	0.0	0.0	0.0	0.0	0.0	0.0
40	0.0	0.0	0.0	0.0	0.0	0.0	0.0	0.0
41	0.0	0.0	0.0	0.0	0.0	0.0	0.0	0.0
42	0.0	0.0	0.0	0.0	0.0	0.0	0.0	0.0
43	0.0	0.0	0.0	0.0	0.0	0.0	0.0	0.0
44	0.0	0.0	0.0	0.0	0.0	0.0	0.0	0.0
45	0.0	0.0	0.0	0.0	0.0	0.0	0.0	0.0
46	0.0	0.0	0.0	0.0	0.0	0.0	0.0	0.0

**Eugene H.  
Lambert  
Ph.D., M.A.**



Table A-4. Continued

Nominal stress $f'_c$	$\beta$	Optimal values						Reduced flexure load $P$	Length $L$
		$f'_s$	$f'_y$	$f'_x$	$f'_z$	$f'_w$	$f'_v$		
2.0	0.5	.75	0.0	0.0	0.0	0.0	0.0	12.073	2.5
		24.0	15.5	26.7	26.6	20.3	27.0	12.073	
		.70	.30	1	.70	.10	.70	12.073	2.5
		21.0	22.0	22.1	22.3	22.0	21.6	12.073	
1.0	0.5	.70	.30	.00	.30	.14	.10	8.283	2.5
		11.073	12.0	15.3	15.3	12.3	12.6	8.283	
		.60	0.0	0.0	0.0	0.0	.60	0.0487	2.5
		21.0	12.0	21.5	21.1	20.3	21.0	0.0487	

As indicated



Fig. 1.1(a) - Co-ordinate System &amp; Filter orientation



Fig. 1.1(b) - Stacking sequence &amp; co-ordinate system for the layered plates.



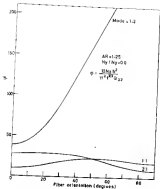


FIG. 2. VARIATION OF BUCKLING LOAD WITH FIBER ORIENTATION

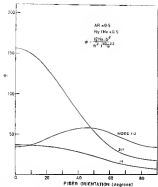


FIG. 2-3 VARIATION OF BUCKLING LOAD WITH FIBER ORIENTATION

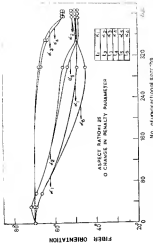


FIG. 2.4. CHANGE IN FIBER ORIENTATION DURING - PHASE 2 - III

## OPTIMAL DESIGN TO FIND OF COMPOSITE PLATES UNDER

### IN-PLANE AND COMPRESSION LOADS.

#### 3.1. INTRODUCTION

Minimum structural weight has been considered as an important criterion for structural design in aerospace engineering applications. The advantages of composites are that they exhibit higher strength to weight ratios than metals, and have better fatigue and corrosion properties. These desirable features have resulted in an increasing use of composites in aerospace structures. Weight saving by replacing metal by composites could lead to considerable fuel saving. Besides minimum weight requirement, aircraft structures are often designed for stiffness, strength, low deflection and high buckling loads.

In chapter 2, an optimal design of composite plates to withstand maximum in-plane compressive loads was discussed. In this chapter, an optimal weight design of composite plates is carried out. The composite plate is subjected to requirements on deflection under transverse loading, and high buckling strength under in-plane compressive loads. The study is carried out for following cases :

- (i) Optimisation of weight of a composite plate under a low deflection requirement.
- (ii) Optimisation of weight of composite plate under a high bending load requirement and minimum deflection.

The first case is considered to understand the behaviour of deflection requirements under transverse loading. Behaviour of a plate under compressive loads is independently studied in Chapter 2. Stresses in plate remain within ultimate values for all fiber orientations and hence constraints on stresses are deleted during the optimisation procedure, and an analysis is carried out at the optimum point.

### 2.1.2 Problem Formulation

Weight per unit area per unit density of composite material is optimised to facilitate a parametric study.

$$\text{Min } W' \Rightarrow \text{Min } \sum_{i=1}^N \frac{V_i}{V} \rho_i \quad (50)$$

where  $W' = \frac{W}{A}$

such that

$$0 \leq \theta_i \leq \pi/2 \quad ; \quad \rho_i \geq 0 \quad i=1, N$$

$$\omega \leq \omega^0$$

$$v_{xx} = \frac{\partial^2 v}{\partial x^2}$$

Constraints are suitably modified to fit into the interior penalty function formulation. An expression for buckling load is obtained in chapter 2 (Eq. (10)). In the following sections, expressions for residual deflection and stresses are obtained.

### 2.3. ANALYSIS

The governing Equations (5.6 and 7) contain distributed except, <sup>(10)</sup> term  $(B_x v_{xx} + B_y v_{yy})$  is replaced by  $-q$ , the intensity of applied transverse load, in Eq. (7).

$$\begin{aligned} D_{11} v_{xxxx} + 2(D_{12} + 2D_{66}) v_{xx yy} + D_{22} v_{yyyy} \\ - B_{11} v_{xx} - (B_{12} + 2B_{66}) v_{yy} - (B_{13} + 2B_{66}) v_{xxy} \\ - 2B_{23} v_{yyy} = q \end{aligned}$$

The deflection of the simply supported plate is obtained by substituting Eq. (9) in Eqs. (5.6 and 7) accordingly.

$$\begin{vmatrix} -\frac{D_{11}}{a^2} & -\frac{D_{12}}{a^2} & \frac{D_{13}}{a^2} \\ \frac{D_{12}}{a^2} & -\frac{D_{22}}{a^2} & \frac{D_{23}}{a^2} \\ -\frac{D_{13}}{a^2} & -\frac{D_{23}}{a^2} & \frac{D_{33}}{a^2} \end{vmatrix} \begin{Bmatrix} \frac{q}{a^2} \\ \frac{q}{a^2} \\ \frac{q}{a^2} \end{Bmatrix} = \begin{Bmatrix} 0 \\ 0 \\ q_{\text{max}} \end{Bmatrix} \quad (14)$$

$$\text{where } q = \sum \sum q_{mn} \quad \text{and} \quad \frac{q_{11}T_{11}}{A} \quad \text{and} \quad \frac{q_{21}T_{11}}{B}$$

and  $T_{11}$  are as defined in Eq. (11)

$q_{mn}$  for uniform loading is,

$$q_{mn} = \frac{24 q_0}{\pi^2 B^2} \frac{1}{m^2} \quad n = 1, 3, 5, \dots, \quad (32)$$

$$n = 1, 3, 5, \dots$$

where

$q_0$  = applied uniform loading per unit area  
Eq. (31) is solved using Gauss's rule and following expressions are obtained.

$$q_{1m} = \frac{q_0}{4 + \frac{B^2}{A^2}} (T_{22} T_{11} - T_{12} T_{21})$$

$$q_{2m} = \frac{q_0}{4 + \frac{B^2}{A^2}} (T_{11} T_{22} - T_{12} T_{21}) \quad (33)$$

and

$$q_{3m} = \frac{q_0}{4 + \frac{B^2}{A^2}} (T_{22} T_{11} - T_{12} T_{21})$$

where

$$B = \frac{(T_{11} T_{22} - T_{12}^2)}{A^2} \left[ T_{11} + \frac{1 + T_{12} T_{21} T_{22} - T_{22} T_{12}^2 - T_{11} T_{22}^2}{T_{11} T_{22} - T_{12}^2} \right]$$

Adding Eqs.(24) and (25) and using  $\bar{u} = u$  and  $\bar{v} = v$  as obtained in the mid-plane theory

$$\begin{aligned}\bar{\epsilon}_x &= \epsilon_x = u & \bar{\epsilon}_y &= \epsilon_y = v \\ \bar{\epsilon}_{xy} &= \gamma_{xy} = v_x - u_y & \bar{\epsilon}_{xy} &= \gamma_{xy}\end{aligned}\quad (26)$$

where  $u$  and  $v$  are the in-plane deflections at the reference surface, which is mid-surface, in our case, since the reference surface deflections  $u$  and  $v$ , the plate curvatures  $\kappa_{xx}$  and  $\kappa_{yy}$ , and the plate twist  $\kappa_{xy}$  are all identical in any given point in the plate, the stresses at the surface  $x$  in the  $k^{th}$  lamina are given by

$$\begin{Bmatrix} \sigma_x^{(k)} \\ \sigma_y^{(k)} \\ \sigma_{xy}^{(k)} \end{Bmatrix} = \begin{bmatrix} Q_{11}^{(k)} & Q_{12}^{(k)} & 0 \\ Q_{12}^{(k)} & Q_{22}^{(k)} & 0 \\ 0 & 0 & Q_{66}^{(k)} \end{bmatrix} \begin{Bmatrix} \epsilon_x^{(k)} \\ \epsilon_y^{(k)} \\ \gamma_{xy}^{(k)} \end{Bmatrix} \quad (27)$$

### 3.3.2. STRESS AND STRAIN IN THE $k^{th}$ LAMINA, $0 \leq z \leq z_k$

The optimisation algorithm requires the derivatives of stresses and transverse deflection. These are obtained as follows.



Let  $v_1$  be some arbitrary  $1 \times 1$  for the present time.

$$v_1 = v_1 \quad i = 1, \omega^2/2$$

$$\text{and} \quad i = v_1 \quad i = \omega^2/2 + 1, \omega^2$$

substituting eqs. (2) in (1), (3) and differentiating (3) twice and reducing we obtained,

$$\frac{dv_1}{dt} = \frac{v_1}{\omega^2} \left( \frac{2 \frac{d^2 v_{11}}{dt^2} v_{23} + v_{11} \frac{d^2 v_{23}}{dt^2}}{\omega^2} \right)$$

$$= \frac{v_{11}}{\omega^2} v_{23} = v_{11} \frac{d^2 v_{23}}{dt^2} = (v_{23} v_{11} v_{12} v_{13}) \frac{d^2}{dt^2}$$

$$\text{and } (v_{12} v_{13}) \text{ and } (v_{23} v_{13}) \quad (4a)$$

$$\frac{dv_1}{dt} = \frac{v_{11}}{\omega^2} \left( \frac{2 \frac{d^2 v_{11}}{dt^2} v_{23} + v_{11} \frac{d^2 v_{23}}{dt^2}}{\omega^2} - \frac{d^2 v_{11}}{dt^2} v_{12} \right)$$

$$= \frac{v_{11}}{\omega^2} v_{12} = (v_{11} v_{12} v_{13} v_{23}) \frac{d^2}{dt^2} \quad (4b)$$

$$\text{and } (v_{12} v_{13}) \text{ and } (v_{23} v_{13})$$

Let  $x_1$  be scalar variables  $i = 1, 2, 3$

Let the powers be:

$$x_1 = x_2 \quad i = 1, 2, 3$$

$$\text{and} \quad x_1 = x_2 \quad i = 1, 2, 3$$

Substituting eq. (11) in Eqs. (6) and differentiating,

values of  $\dot{x}_1$  and  $\dot{x}_2$  are obtained,

$$\frac{\dot{x}_1}{\dot{x}_2} = \frac{1}{\dot{x}_2} \left( \frac{2 \frac{\partial^2 x_1}{\partial x_1^2} x_2 - \frac{\partial^2 x_1}{\partial x_1^2}}{2} \right)$$

$$\frac{\dot{x}_1}{\dot{x}_2} = \frac{2 \frac{\partial^2 x_1}{\partial x_1^2} x_2 - \frac{\partial^2 x_1}{\partial x_1^2}}{2}$$

$$\cos \theta \left( \frac{\partial^2 x_1}{\partial x_1^2} \right) \sin \theta \left( \frac{\partial^2 x_1}{\partial x_1^2} \right) \quad (12)$$

$$\frac{\dot{x}_1}{\dot{x}_2} = \frac{1}{\dot{x}_2} \left( \frac{2 \frac{\partial^2 x_1}{\partial x_1^2} x_2 - \frac{\partial^2 x_1}{\partial x_1^2}}{2} \right)$$

$$\frac{\dot{x}_1}{\dot{x}_2} = \frac{2 \frac{\partial^2 x_1}{\partial x_1^2} x_2 - \frac{\partial^2 x_1}{\partial x_1^2}}{2} \quad (13)$$

$$\sin \theta \left( \frac{\partial^2 x_1}{\partial x_1^2} \right) \cos \theta \left( \frac{\partial^2 x_1}{\partial x_1^2} \right)$$

$$\frac{\partial \pi}{\partial \sigma_1} = \frac{\partial \pi}{\partial \sigma_1} \left[ 2 \left( \frac{\partial \pi_{12}}{\partial \sigma_1} - \tau_{11} + \tau_{12} \frac{\partial \tau_{11}}{\partial \sigma_1} - 2 \tau_{12} \frac{\partial \tau_{12}}{\partial \sigma_1} \right) \right. \\ \left. - (\tau_{22} - \tau_{12} - \tau_{11}^2) \frac{\partial \sigma}{\partial \sigma_1} \right] \quad (16)$$

where

$$\frac{\partial \sigma}{\partial \sigma_1} = \frac{1}{\sigma} \left( \frac{\partial \tau_{11}}{\partial \sigma_1} \tau_{11} + \tau_{11} \frac{\partial \tau_{12}}{\partial \sigma_1} - 2 \tau_{12} \frac{\partial \tau_{12}}{\partial \sigma_1} \right) \\ \left[ \frac{\partial \tau_{12}}{\partial \sigma_1} + \left\{ (\tau_{11} \tau_{12} - \tau_{12}^2) + 2 \frac{\partial \tau_{12}}{\partial \sigma_1} \tau_{22} \tau_{12} + 2 \frac{\partial \tau_{12}}{\partial \sigma_1} \tau_{12} \tau_{13} + \tau_{12} \tau_{13} + 2 \frac{\partial \tau_{13}}{\partial \sigma_1} \tau_{12} \tau_{13} - \frac{\partial \tau_{22}}{\partial \sigma_1} \tau_{12}^2 - 2 \frac{\partial \tau_{13}}{\partial \sigma_1} \tau_{22} \tau_{12} \right. \right. \\ \left. \left. + \frac{\partial \tau_{11}}{\partial \sigma_1} \tau_{22}^2 + 2 \frac{\partial \tau_{22}}{\partial \sigma_1} \tau_{12} \right. \right. \\ \left. \left. + (\tau_{12} \tau_{13} \tau_{12} - \tau_{12}^2 \tau_{13} - \tau_{12} \tau_{13}^2 - \tau_{12}^2 \tau_{22}) \right\} \right] \\ \left( \frac{\partial \tau_{11}}{\partial \sigma_1} \tau_{22} + \frac{\partial \tau_{12}}{\partial \sigma_1} \tau_{12} - 2 \frac{\partial \tau_{12}}{\partial \sigma_1} \tau_{12} \right) / \\ \left( \tau_{11} \tau_{12} - \tau_{12}^2 \right)^2 \Bigg] \Bigg\}$$

and

$$\frac{\partial \tau_{11}}{\partial \sigma_1} \quad \text{are given by Eq. (13)}$$

Gradients of stresses can be obtained in the following manner :

$$\begin{aligned} \frac{\partial \sigma_{ij}^{(k)}}{\partial v_j} &= \lambda \frac{\partial \sigma_{ij}^{(k)}}{\partial v_j} + \frac{\partial \sigma_{ij}^{(k)}}{\partial v_j} \frac{\partial v_j}{\partial v_j} \quad i = 1, 2, \text{ and } 3 \\ &\quad i = 1, 2 \text{ and } 3 \\ &\quad j = 1, 2 \end{aligned} \quad (60)$$

where

$$\begin{aligned} \frac{\partial \sigma_{ij}^{(k)}}{\partial v_j} &= \frac{\partial \sigma_{ij}^{(k)}}{\partial v_j} = \lambda \frac{\partial \sigma_{ij}^{(k)}}{\partial v_j} + \frac{\partial \sigma_{ij}^{(k)}}{\partial v_j} v_{ij} \\ \frac{\partial \sigma_{ij}^{(k)}}{\partial v_j} &= \frac{\partial \sigma_{ij}^{(k)}}{\partial v_j} = \lambda \frac{\partial \sigma_{ij}^{(k)}}{\partial v_j} + \frac{\partial \sigma_{ij}^{(k)}}{\partial v_j} v_{ij} \end{aligned} \quad (61)$$

$$\frac{\partial \sigma_{ij}^{(k)}}{\partial v_j} = \frac{\partial \sigma_{ij}^{(k)}}{\partial v_j} + \frac{\partial \sigma_{ij}^{(k)}}{\partial v_j} = \lambda \frac{\partial \sigma_{ij}^{(k)}}{\partial v_j} + \frac{\partial \sigma_{ij}^{(k)}}{\partial v_j} v_{ij}$$

Derivatives of  $\{\sigma_{ij}^{(k)}\}$  and  $\lambda$  are given in Appendix - 1 .

### 3.3.4. CONSTRAINTS AND THEIR GRADIENTS

Constraints and their derivatives for the optimisation studies are obtained as follows.

The set of constraints described by Eqs. (14-16) in chapter 2 are also applied to minimise weight

optimization problem considered here. Their derivatives are given by Eqs. (17, 18 and 22). In addition to these constraints, constraints on the major  $\sigma$  direction and the ultimate stresses in principal directions or Tsai - Hill yield criterion for anisotropic materials, are applied in the first problem. Second problem includes constraint on buckling in addition to the constraints imposed on the first problem.

The additional constraints are

$$g_1 = 1 - \sigma^2/\sigma_x^2 \quad (42)$$

$$g_2 = (\sigma_x/\sigma_x^0) - 1 \quad (43)$$

$$g_3 = 1 + \frac{\sigma_{33}^2}{\sigma_x^2} \quad i = 3, 3+1 \quad (44)$$

$$g_4 = 1 - \frac{\sigma_y^2 + \sigma_{xy}^2}{\sigma_y^2} \quad i=4, 2M+4 \quad (45)$$

$$g_5 = 1 - \frac{\sigma_{xy}^2 + \sigma_{yz}^2}{\sigma_{xy}^2} \quad i=2M+5, 2M+6 \quad (46)$$

and

$$g_6 = 1 - \left( \frac{\sigma_{33}^2}{\sigma_x^2} \right)^2 + \frac{\sigma_{33}^2}{\sigma_x^2} \frac{\sigma_{33}^2}{\sigma_x^2} + \left( \frac{\sigma_y^2}{\sigma_y^0} \right)^2 - \left( \frac{\sigma_{xy}^2}{\sigma_y^0} \right)^2 \quad i = 3, 3+1 \quad (47)$$

where

$$\begin{Bmatrix} \sigma_x^0 \\ \sigma_y^0 \\ \sigma_{xy}^0 \end{Bmatrix} = [T]^{-1} \begin{Bmatrix} \sigma_{120} \\ \sigma_{20} \\ \sigma_{120} \end{Bmatrix} \quad (58)$$

where

$$[T]^{-1} = [T]^T = \begin{bmatrix} \cos^2 \alpha & \sin^2 \alpha & -2 \sin \alpha \cos \alpha \\ \sin^2 \alpha & \cos^2 \alpha & 2 \sin \alpha \cos \alpha \\ 2 \sin \alpha \cos \alpha & -2 \sin \alpha \cos \alpha & (\cos^2 \alpha - \sin^2 \alpha) \end{bmatrix} \quad (59)$$

It should be noted that the fibers at orientations  $+\alpha$  and  $-\alpha$  will contribute to the ultimate strength in the principal directions, therefore,

$$\begin{aligned} \sigma_x^0 &= \sigma_{120} \sin^2 \alpha + \sigma_{20} \cos^2 \alpha \\ \sigma_y^0 &= \sigma_{120} \sin^2 \alpha + \sigma_{20} \cos^2 \alpha \\ \sigma_{xy}^0 &= \sigma_{120} (\cos^2 \alpha - \sin^2 \alpha) \end{aligned} \quad (60)$$

Derivatives of constraints are

$$\frac{\partial g_1}{\partial x_1} = -\frac{1}{v^2} \frac{\partial v}{\partial x_1} \quad i = 1, N \quad (61)$$

$$\frac{\partial g_2}{\partial x_1} = -\frac{1}{v^2} \frac{\partial v}{\partial x_1} \quad i = 1, N \quad (62)$$

$$\frac{\partial v_1}{\partial v_j} = - \frac{1}{\frac{1}{\sigma}} \frac{\partial \sigma_{\frac{1}{2}(1-1)}^{\frac{1}{2}}}{\partial v_j} \quad \begin{matrix} i=1, 1+1 \\ j=1, N' \end{matrix} \quad (73)$$

$$\frac{\partial v_2}{\partial v_j} = - \frac{1}{\frac{1}{\sigma}} \frac{\partial \sigma_{\frac{1}{2}(2-1)(1-1)}^{\frac{1}{2}}}{\partial v_j} \quad \begin{matrix} i=2+1, 1+1 \\ j=1, N' \end{matrix} \quad (74)$$

$$\frac{\partial v_3}{\partial v_j} = - \frac{1}{\frac{1}{\sigma}} \frac{\partial \sigma_{\frac{1}{2}(3-1-1)(2-1)}^{\frac{1}{2}}}{\partial v_j} \quad \begin{matrix} i=3+1, 2+1 \\ j=1, N' \end{matrix} \quad (75)$$

or

$$\begin{aligned} \frac{\partial v_1}{\partial v_j} &= - : \frac{\sigma_{\frac{1}{2}(1-1)}^{\frac{1}{2}}}{\sigma^{\frac{1}{2}}} \frac{\partial \sigma_{\frac{1}{2}(1-1)}^{\frac{1}{2}}}{\partial v_j} + \frac{\sigma_{\frac{1}{2}(1-1)}^{\frac{1}{2}}}{\sigma^{\frac{1}{2}}} \frac{\partial \sigma_{\frac{1}{2}(1-1)}^{\frac{1}{2}}}{\partial v_j} \\ &= \frac{\sigma_{\frac{1}{2}(1-1)}^{\frac{1}{2}}}{\sigma^{\frac{1}{2}}} \frac{\partial \sigma_{\frac{1}{2}(1-1)}^{\frac{1}{2}}}{\partial v_j} = \frac{\sigma_{\frac{1}{2}(1-1)}^{\frac{1}{2}}}{\sigma^{\frac{1}{2}}} \frac{\partial \sigma_{\frac{1}{2}(1-1)}^{\frac{1}{2}}}{\partial v_j} \\ &\quad \begin{matrix} i = 1, 1+1 \\ j = 1, N' \end{matrix} \end{aligned} \quad (76)$$

## 2.4. ANALYSIS AND DISCUSSION

### 2.4.1. ANALYSIS

Minimum weight optimization of a rectangular plate has been carried out for varying values of plate and support ratios, for known/known conditions, whose material properties are as given in section(2.4.1).

$$\frac{\partial v_j}{\partial v_j} = - \frac{1}{v_j} \frac{\partial \sigma_{j+1}}{\partial v_j} \quad (1 \leq j \leq n-1, \quad j=1, 2^*) \quad (72)$$

$$\frac{\partial v_j}{\partial v_j} = - \frac{1}{v_j} \frac{\partial \sigma_{j+1}}{\partial v_j} \quad (1 \leq j \leq n-1, \quad j=1, 2^*) \quad (73)$$

$$\frac{\partial v_j}{\partial v_j} = - \frac{1}{v_j} \frac{\partial \sigma_{j+1}}{\partial v_j} \quad (1 \leq j \leq n-1, \quad j=1, 2^*) \quad (74)$$

40

$$\begin{aligned} \frac{\partial v_j}{\partial v_j} = & - \frac{\sigma_{j+1}}{v_j} \frac{\partial \sigma_{j+1}}{\partial v_j} + \frac{\sigma_{j+1}}{v_j} \frac{\partial \sigma_{j+1}}{\partial v_j} \\ & + \frac{\sigma_{j+1}}{v_j} \frac{\partial \sigma_{j+1}}{\partial v_j} - \frac{\sigma_{j+1}}{v_j} \frac{\partial \sigma_{j+1}}{\partial v_j} \\ & i = 2, 3, \dots \\ & j = 1, 2^* \end{aligned} \quad (75)$$

## 1.4. ANALYSIS AND DESIGN

### 2.4.1. ANALYSIS

Minimum weight optimization of a rectangular plate has been carried out. The representation of plate and support points, and beam/rod elements, using material properties are as given in section(2.4.1).



Arterial pressure has been compared for the following set of conditions:

Longitudinal velocity growth =  $1.0 \times 10^3$  km/deg.yr.

Transverse basella segment = 0.40 mm/seg.

Longitudinal compressive strength: 200–1.5



*Tasmanian conifers* [abstracts](#)—2013 448p, 00.

Received 17 February 2003; accepted 10 June 2003

Applied and Numerical Harmonic Analysis, 1 (2014) 1–10

100

Upper limit on maximum deflection: 0.6 mm.

Kijewski buckling load in  $x$ -directions,  $N_{xcr}$ .

Table 3.1 presents the optimum ply thickness and corresponding fiber orientation for a minimum weight design of a plate subjected to uniform transverse loading. The application of the plate is restricted to be within prescribed upper limit. Results for different aspect ratios are tabulated. For each aspect ratio, a plate with varying number of ply is considered.

The variation of the maximum deflection with fiber orientation is plotted in Fig. 3.1. The values of the maximum deflection of the plate is obtained as:

higher fiber orientations as aspect ratio increases. The rate of increase decreases as well for plates of low aspect ratio while for plates of higher aspect ratios, it increases rapidly.

Figs. 3.2.3.3 and 3.4) show the variations of stresses in positive fiber directions (compressive in fiber direction, and shear stress with fiber are positive, respectively).

The optimum ply thickness and corresponding fiber orientations for plates with varying aspect ratio and biaxial loading ratio are presented in Table 3.1. Optimum fiber orientation angle increases with an increase in biaxial loading ratio for lower aspect ratios. The change is small as aspect ratio approaches unity. For a square plate the fiber orientation angle reaches 45 deg. (45°) with increase in biaxial loading ratio. The contribution of ply thickness near mid-plane is not considerable. In fact, the fiber orientation of the plies near mid-plane do not achieve an optimum orientation, but their effect is nullified, as an extent, by reducing the thickness to an almost negligible value.



Eq. (2.4) is changing off the variables to the nearest available value. Figs. 3.3-3.4) consist the results of the analysis. Fig. 3.3 contains the variation of the maximum deflection, reflection of composite plate with fiber orientation. Variation of stress in positive fiber direction, stress increases in positive fiber direction, and shear stress ( $\sigma_{xy}$ ), with fiber orientation is shown in Fig. 3.3, Fig. 3.3 and Fig. 3.4, respectively.

The requirement on deflection is very stringent in all aerospace designs. Stiffer subcarrier or buckling is the governing design criterion has appeared as well as the uniform while if the design remains within the requirements for deflection and stability. Figs. 3.3-3.4) indicates this behavior. (Carbon filaments have a high modulus and high strength and low density. Kevlar filaments are often designed for stiffness and fiber, and some fiber is particularly suitable for low deflection and high strength applications.) And as the variation on stress or strength condition is varied relative to the optimum, these constraints are relaxed during optimization procedure and only analysis is done at the final optimum point.

Eq. (2.4) and Eq. (2.5) show that the factor

$$1/\pi^2 \cdot \pi^2 \left\{ \sigma^2 + \sigma_0^2 \left( \sigma_0/\sigma_0 \right)^2 \right\}$$

appears in the expression and  $\delta_{x,ave}$  is  $\delta_{x,ave}$  appears in the expression for the transverse deflection. It seems that at lower aspect ratios, bending will be the governing criterion, while at higher aspect ratios, the deflection will be an active constraint. With higher values of lateral loading, the changeover from buckling to deflection as an active constraint will take place at still higher aspect ratios. Analysis, similar to that of a in section (3.4.1) will substantiate the results obtained for the optimum fiber orientations in table 3.1. The reasons given for the variations of ply thickness, at the end of section (3.4.2), hold good for results presented in table 3.1 and table 3.3.

The optimum weight does not depend upon the lateral loading ratio if the constraint on deflection is active. It increases with increase in lateral loading ratio because the buckling load decreases with increasing lateral loading ratio and, hence, the thickness of the laminate has to compensate for it so get the design to satisfy the stability requirement (eq. 3.7).

### 3.5 CONCLUSIONS

The following conclusions can be drawn.

- (1) The weight per unit area of the plate increases with increasing aspect ratio. However, it seems to approach an asymptotic value with aspect ratio.

- (2) Stability criterion is the square constraint at lower output levels. The transient deflection is the active constraint at higher output levels.
- (3) The design, from the stability criterion to the deflection criterion as an active constraint, takes place at higher output levels with increase in torque, loading.
- (4) Stiffness never become active at optimum point with the deflection requirement at the last two cases. These constraints can be deleted to improve the efficiency of the algorithm.

Conclusions given at the end of chapter 3, in general, hold for the random weight design under approximate deflection and stability constraints, too.

Table 2.1 = 70% Official and 30% of 70% = 42% (approximately) as

© 2004 Blackwell Publishing Ltd *Journal of Internal Medicine* 255: 103–110

1997, 1998, 1999, 2000, 2001, 2002, 2003, 2004, 2005, 2006, 2007, 2008, 2009, 2010, 2011, 2012, 2013, 2014, 2015, 2016, 2017, 2018, 2019, 2020, 2021, 2022, 2023, 2024, 2025, 2026, 2027, 2028, 2029, 2030, 2031, 2032, 2033, 2034, 2035, 2036, 2037, 2038, 2039, 2040, 2041, 2042, 2043, 2044, 2045, 2046, 2047, 2048, 2049, 2050, 2051, 2052, 2053, 2054, 2055, 2056, 2057, 2058, 2059, 2060, 2061, 2062, 2063, 2064, 2065, 2066, 2067, 2068, 2069, 2070, 2071, 2072, 2073, 2074, 2075, 2076, 2077, 2078, 2079, 2080, 2081, 2082, 2083, 2084, 2085, 2086, 2087, 2088, 2089, 2090, 2091, 2092, 2093, 2094, 2095, 2096, 2097, 2098, 2099, 2100, 2101, 2102, 2103, 2104, 2105, 2106, 2107, 2108, 2109, 2110, 2111, 2112, 2113, 2114, 2115, 2116, 2117, 2118, 2119, 2120, 2121, 2122, 2123, 2124, 2125, 2126, 2127, 2128, 2129, 2130, 2131, 2132, 2133, 2134, 2135, 2136, 2137, 2138, 2139, 2140, 2141, 2142, 2143, 2144, 2145, 2146, 2147, 2148, 2149, 2150, 2151, 2152, 2153, 2154, 2155, 2156, 2157, 2158, 2159, 2160, 2161, 2162, 2163, 2164, 2165, 2166, 2167, 2168, 2169, 2170, 2171, 2172, 2173, 2174, 2175, 2176, 2177, 2178, 2179, 2180, 2181, 2182, 2183, 2184, 2185, 2186, 2187, 2188, 2189, 2190, 2191, 2192, 2193, 2194, 2195, 2196, 2197, 2198, 2199, 2200, 2201, 2202, 2203, 2204, 2205, 2206, 2207, 2208, 2209, 2210, 2211, 2212, 2213, 2214, 2215, 2216, 2217, 2218, 2219, 2220, 2221, 2222, 2223, 2224, 2225, 2226, 2227, 2228, 2229, 2230, 2231, 2232, 2233, 2234, 2235, 2236, 2237, 2238, 2239, 2240, 2241, 2242, 2243, 2244, 2245, 2246, 2247, 2248, 2249, 2250, 2251, 2252, 2253, 2254, 2255, 2256, 2257, 2258, 2259, 2260, 2261, 2262, 2263, 2264, 2265, 2266, 2267, 2268, 2269, 2270, 2271, 2272, 2273, 2274, 2275, 2276, 2277, 2278, 2279, 2280, 2281, 2282, 2283, 2284, 2285, 2286, 2287, 2288, 2289, 2290, 2291, 2292, 2293, 2294, 2295, 2296, 2297, 2298, 2299, 2300, 2301, 2302, 2303, 2304, 2305, 2306, 2307, 2308, 2309, 2310, 2311, 2312, 2313, 2314, 2315, 2316, 2317, 2318, 2319, 2320, 2321, 2322, 2323, 2324, 2325, 2326, 2327, 2328, 2329, 2330, 2331, 2332, 2333, 2334, 2335, 2336, 2337, 2338, 2339, 2340, 2341, 2342, 2343, 2344, 2345, 2346, 2347, 2348, 2349, 2350, 2351, 2352, 2353, 2354, 2355, 2356, 2357, 2358, 2359, 2360, 2361, 2362, 2363, 2364, 2365, 2366, 2367, 2368, 2369, 2370, 2371, 2372, 2373, 2374, 2375, 2376, 2377, 2378, 2379, 2380, 2381, 2382, 2383, 2384, 2385, 2386, 2387, 2388, 2389, 2390, 2391, 2392, 2393, 2394, 2395, 2396, 2397, 2398, 2399, 2400, 2401, 2402, 2403, 2404, 2405, 2406, 2407, 2408, 2409, 2410, 2411, 2412, 2413, 2414, 2415, 2416, 2417, 2418, 2419, 2420, 2421, 2422, 2423, 2424, 2425, 2426, 2427, 2428, 2429, 2430, 2431, 2432, 2433, 2434, 2435, 2436, 2437, 2438, 2439, 2440, 2441, 2442, 2443, 2444, 2445, 2446, 2447, 2448, 2449, 2450, 2451, 2452, 2453, 2454, 2455, 2456, 2457, 2458, 2459, 2460, 2461, 2462, 2463, 2464, 2465, 2466, 2467, 2468, 2469, 2470, 2471, 2472, 2473, 2474, 2475, 2476, 2477, 2478, 2479, 2480, 2481, 2482, 2483, 2484, 2485, 2486, 2487, 2488, 2489, 2490, 2491, 2492, 2493, 2494, 2495, 2496, 2497, 2498, 2499, 2500, 2501, 2502, 2503, 2504, 2505, 2506, 2507, 2508, 2509, 2510, 2511, 2512, 2513, 2514, 2515, 2516, 2517, 2518, 2519, 2520, 2521, 2522, 2523, 2524, 2525, 2526, 2527, 2528, 2529, 2530, 2531, 2532, 2533, 2534, 2535, 2536, 2537, 2538, 2539, 2540, 2541, 2542, 2543, 2544, 2545, 2546, 2547, 2548, 2549, 2550, 2551, 2552, 2553, 2554, 2555, 2556, 2557, 2558, 2559, 2560, 2561, 2562, 2563, 2564, 2565, 2566, 2567, 2568, 2569, 2570, 2571, 2572, 2573, 2574, 2575, 2576, 2577, 2578, 2579, 2580, 2581, 2582, 2583, 2584, 2585, 2586, 2587, 2588, 2589, 2590, 2591, 2592, 2593, 2594, 2595, 2596, 2597, 2598, 2599, 2600, 2601, 2602, 2603, 2604, 2605, 2606, 2607, 2608, 2609, 2610, 2611, 2612, 2613, 2614, 2615, 2616, 2617, 2618, 2619, 2620, 2621, 2622, 2623, 2624, 2625, 2626, 2627, 2628, 2629, 2630, 2631, 2632, 2633, 2634, 2635, 2636, 2637, 2638, 2639, 2640, 2641, 2642, 2643, 2644, 2645, 2646, 2647, 2648, 2649, 2650, 2651, 2652, 2653, 2654, 2655, 2656, 2657, 2658, 2659, 2660, 2661, 2662, 2663, 2664, 2665, 2666, 2667, 2668, 2669, 2670, 2671, 2672, 2673, 2674, 2675, 2676, 2677, 2678, 26

[illegible]

**1993-2000**

Run No.	Time	Temp. (°C)	Pressure (mm Hg)	Volume (ml)	Weight (g)	Calculated
1	0.00	0.00	0.00	0.00	0.00	0.00
2	0.01	0.01	0.01	0.01	0.01	0.01
3	0.02	0.02	0.02	0.02	0.02	0.02
4	0.03	0.03	0.03	0.03	0.03	0.03
5	0.04	0.04	0.04	0.04	0.04	0.04
6	0.05	0.05	0.05	0.05	0.05	0.05
7	0.06	0.06	0.06	0.06	0.06	0.06
8	0.07	0.07	0.07	0.07	0.07	0.07
9	0.08	0.08	0.08	0.08	0.08	0.08
10	0.09	0.09	0.09	0.09	0.09	0.09
11	0.10	0.10	0.10	0.10	0.10	0.10
12	0.11	0.11	0.11	0.11	0.11	0.11
13	0.12	0.12	0.12	0.12	0.12	0.12
14	0.13	0.13	0.13	0.13	0.13	0.13
15	0.14	0.14	0.14	0.14	0.14	0.14
16	0.15	0.15	0.15	0.15	0.15	0.15
17	0.16	0.16	0.16	0.16	0.16	0.16
18	0.17	0.17	0.17	0.17	0.17	0.17
19	0.18	0.18	0.18	0.18	0.18	0.18
20	0.19	0.19	0.19	0.19	0.19	0.19
21	0.20	0.20	0.20	0.20	0.20	0.20
22	0.21	0.21	0.21	0.21	0.21	0.21
23	0.22	0.22	0.22	0.22	0.22	0.22
24	0.23	0.23	0.23	0.23	0.23	0.23
25	0.24	0.24	0.24	0.24	0.24	0.24
26	0.25	0.25	0.25	0.25	0.25	0.25
27	0.26	0.26	0.26	0.26	0.26	0.26
28	0.27	0.27	0.27	0.27	0.27	0.27
29	0.28	0.28	0.28	0.28	0.28	0.28
30	0.29	0.29	0.29	0.29	0.29	0.29
31	0.30	0.30	0.30	0.30	0.30	0.30
32	0.31	0.31	0.31	0.31	0.31	0.31
33	0.32	0.32	0.32	0.32	0.32	0.32
34	0.33	0.33	0.33	0.33	0.33	0.33
35	0.34	0.34	0.34	0.34	0.34	0.34
36	0.35	0.35	0.35	0.35	0.35	0.35
37	0.36	0.36	0.36	0.36	0.36	0.36
38	0.37	0.37	0.37	0.37	0.37	0.37
39	0.38	0.38	0.38	0.38	0.38	0.38
40	0.39	0.39	0.39	0.39	0.39	0.39
41	0.40	0.40	0.40	0.40	0.40	0.40
42	0.41	0.41	0.41	0.41	0.41	0.41
43	0.42	0.42	0.42	0.42	0.42	0.42
44	0.43	0.43	0.43	0.43	0.43	0.43
45	0.44	0.44	0.44	0.44	0.44	0.44
46	0.45	0.45	0.45	0.45	0.45	0.45
47	0.46	0.46	0.46	0.46	0.46	0.46
48	0.47	0.47	0.47	0.47	0.47	0.47
49	0.48	0.48	0.48	0.48	0.48	0.48
50	0.49	0.49	0.49	0.49	0.49	0.49
51	0.50	0.50	0.50	0.50	0.50	0.50
52	0.51	0.51	0.51	0.51	0.51	0.51
53	0.52	0.52	0.52	0.52	0.52	0.52
54	0.53	0.53	0.53	0.53	0.53	0.53
55	0.54	0.54	0.54	0.54	0.54	0.54
56	0.55	0.55	0.55	0.55	0.55	0.55
57	0.56	0.56	0.56	0.56	0.56	0.56
58	0.57	0.57	0.57	0.57	0.57	0.57
59	0.58	0.58	0.58	0.58	0.58	0.58
60	0.59	0.59	0.59	0.59	0.59	0.59
61	0.60	0.60	0.60	0.60	0.60	0.60
62	0.61	0.61	0.61	0.61	0.61	0.61
63	0.62	0.62	0.62	0.62	0.62	0.62
64	0.63	0.63	0.63	0.63	0.63	0.63
65	0.64	0.64	0.64	0.64	0.64	0.64
66	0.65	0.65	0.65	0.65	0.65	0.65
67	0.66	0.66	0.66	0.66	0.66	0.66
68	0.67	0.67	0.67	0.67	0.67	0.67
69	0.68	0.68	0.68	0.68	0.68	0.68
70	0.69	0.69	0.69	0.69	0.69	0.69
71	0.70	0.70	0.70	0.70	0.70	0.70
72	0.71	0.71	0.71	0.71	0.71	0.71
73	0.72	0.72	0.72	0.72	0.72	0.72
74	0.73	0.73	0.73	0.73	0.73	0.73
75	0.74	0.74	0.74	0.74	0.74	0.74
76	0.75	0.75	0.75	0.75	0.75	0.75
77	0.76	0.76	0.76	0.76	0.76	0.76
78	0.77	0.77	0.77	0.77	0.77	0.77
79	0.78	0.78	0.78	0.78	0.78	0.78
80	0.79	0.79	0.79	0.79	0.79	0.79
81	0.80	0.80	0.80	0.80	0.80	0.80
82	0.81	0.81	0.81	0.81	0.81	0.81
83	0.82	0.82	0.82	0.82	0.82	0.82
84	0.83	0.83	0.83	0.83	0.83	0.83
85	0.84	0.84	0.84	0.84	0.84	0.84
86	0.85	0.85	0.85	0.85	0.85	0.85
87	0.86	0.86	0.86	0.86	0.86	0.86
88	0.87	0.87	0.87	0.87	0.87	0.87
89	0.88	0.88	0.88	0.88	0.88	0.88
90	0.89	0.89	0.89	0.89	0.89	0.89
91	0.90	0.90	0.90	0.90	0.90	0.90
92	0.91	0.91	0.91	0.91	0.91	0.91
93	0.92	0.92	0.92	0.92	0.92	0.92
94	0.93	0.93	0.93	0.93	0.93	0.93
95	0.94	0.94	0.94	0.94	0.94	0.94
96	0.95	0.95	0.95	0.95	0.95	0.95
97	0.96	0.96	0.96	0.96	0.96	0.96
98	0.97	0.97	0.97	0.97	0.97	0.97
99	0.98	0.98	0.98	0.98	0.98	0.98
100	0.99	0.99	0.99	0.99	0.99	0.99
101	1.00	1.00	1.00	1.00	1.00	1.00



TABLE 3-1. CONTINUED

Design load area	Design pitch	Optimal values					Optimal weight lb/in. <sup>2</sup>
		$V_{x1}$	$V_{x2}$	$V_{y1}$	$V_{y2}$	$V_{y3}$	
2.0	7	8.53	2.97				4.69
		99.79	99.79				
4	8	4.45	0.13	9.41	2.53		4.69
		99.7	10.28	91.22	99.69		
6	9	2.33	0.13	4.43	0.13	0.13	5.09
		99.12	93.89	47.69	47.99	93.90	



TABLE 1.7. CONTINUED

Amount fed to cows	$\bar{Y}_i$	No. of plots	Quantities of nutrients fed				Optimum weight kg/A
			$Y_{i1}$	$Y_{i2}$	$Y_{i3}$	$Y_{i4}$	
0.5	0.5	2	1.45	1.45			2.55
			23.43	23.33			
		4	1.35	0.60	0.60	1.55	2.08
			28.1	55.8	51.0	33.8	
0.0	0.0	2	1.65	1.70			3.35
			37.5	37.85			
		4	1.68	0.35	0.35	1.58	2.29
			37.7	42.67	42.09	37.62	
0.5	0.5	2	1.72	1.72			3.44
			40.0	40.00			
0.0	0.0	2	1.72	0.71		1.71	2.68
			39.27	42.24	42.23	37.4	

Table 1.1. Continued

Approximate water depth $\frac{h}{m}$	No. of plugs	Between 0.5 and 1.0 m				Optimum water depth $\frac{h}{m}$
		$\frac{v}{v_{cr}}$	$\frac{v}{v_{gr}}$	$\frac{v}{v_{pr}}$	$\frac{v}{v_{cr}}$	
1.0	8	1.00	1.00	—	—	2.10
		0.00	20.00	—	—	
0.9	4	1.00	0.00	0.00	0.00	2.70
		15.87	61.00	45.00	37.00	
0.8	7	1.00	1.00	—	—	4.80
		37.00	37.00	—	—	
0.7	8	1.00	0.00	0.00	0.00	3.80
		07.00	44.00	42.00	35.00	
0.6	8	1.00	0.00	—	—	6.00
		05.00	09.00	—	—	
0.5	1	1.00	1.00	0.00	0.00	5.00
		00.00	05.00	05.00	0.00	
0.3	2	2.00	2.00	—	—	1.00
		05.00	05.00	—	—	

DATA FOR CORRELATION

No. of specimens tested	Distances from base, in.				No. of plates	$\frac{P}{A}$	Average ratio $\frac{P}{P_y}$
	$C_{1/4}$	$C_{1/2}$	$C_{3/4}$	$C_{full}$			
4	1.00	1.00	1.00	1.00	4	8.5	0.5
4	1.00	0.50	0.50	0.50	4	8.0	0.5
	1.00	0.50	0.50	0.50			
	1.00	1.00	1.00	1.00			
	0.50	0.50	0.50	0.50			
4	1.00	1.00	1.00	1.00	4	8.0	0.5
4	1.00	0.50	0.50	0.50	4	7.5	0.5
	1.00	0.50	0.50	0.50			
	1.00	1.00	1.00	1.00			
	0.50	0.50	0.50	0.50			
4	1.00	1.00	1.00	1.00	4	7.0	0.5
4	1.00	0.50	0.50	0.50	4	6.5	0.5
	1.00	0.50	0.50	0.50			
	1.00	1.00	1.00	1.00			
	0.50	0.50	0.50	0.50			
4	1.00	1.00	1.00	1.00	4	6.0	0.5
4	1.00	0.50	0.50	0.50	4	5.5	0.5
	1.00	0.50	0.50	0.50			
	1.00	1.00	1.00	1.00			
	0.50	0.50	0.50	0.50			
4	1.00	1.00	1.00	1.00	4	5.0	0.5
4	1.00	0.50	0.50	0.50	4	4.5	0.5
	1.00	0.50	0.50	0.50			
	1.00	1.00	1.00	1.00			
	0.50	0.50	0.50	0.50			
4	1.00	1.00	1.00	1.00	4	4.0	0.5
4	1.00	0.50	0.50	0.50	4	3.5	0.5
	1.00	0.50	0.50	0.50			
	1.00	1.00	1.00	1.00			
	0.50	0.50	0.50	0.50			
4	1.00	1.00	1.00	1.00	4	3.0	0.5
4	1.00	0.50	0.50	0.50	4	2.5	0.5
	1.00	0.50	0.50	0.50			
	1.00	1.00	1.00	1.00			
	0.50	0.50	0.50	0.50			
4	1.00	1.00	1.00	1.00	4	2.0	0.5
4	1.00	0.50	0.50	0.50	4	1.5	0.5
	1.00	0.50	0.50	0.50			
	1.00	1.00	1.00	1.00			
	0.50	0.50	0.50	0.50			
4	1.00	1.00	1.00	1.00	4	1.0	0.5
4	1.00	0.50	0.50	0.50	4	0.5	0.5
	1.00	0.50	0.50	0.50			
	1.00	1.00	1.00	1.00			
	0.50	0.50	0.50	0.50			

TABLE 1.2. CONTINUED

Adjusted depth feet	$\frac{L}{d}$	NO. OF STARS	$\frac{v_1}{K_1}$	$\frac{v_2}{K_2}$	$\frac{v_3}{K_3}$	$\frac{v_4}{K_4}$	Optimum velocity m/sec
0.5	1	7	24.200	24.700			4.57
			50.0	53.0			
			1.74	0.558	0.07	1.10	4.57
1.0	2		53.7	50.3	10.15	50.5	
1.5	3		8.20	4.200			4.57
			52.4	52.5			
			2.13	0.10	0.01	2.00	4.57
2.0	4		52.0	40.4	40.2	52.5	
2.5	5		2.34	2.30			4.57
			52.0	52.0			
			52.6	0.00	0.43	1.70	4.57
3.0	6		52.6	11.7	10.4	52.3	
3.5	7		2.4	2.5			4.57
			52.9	49.8			
			2.15	5.50	0.07	2.10	4.57
4.0	8		52.0	52.0	50.3	50.3	

# Table 2.2 - continued

Project Title	Year 1990	Year 1991	Year 1992	Year 1993	Year 1994	Year 1995
1.01	1.01	1	20.45	21.10		4.00
			14.10	88.10		
			7.10	0.00	0.00	0.00
			88.45	13.11	13.11	88.10
1.02	1	1	1.00	1.01		4.00
			87.10	88.10		
			1.10	0.00	0.00	0.00
			88.10	13.11	13.11	88.10
1.03	1	1	20.45	21.10		4.00
			14.10	88.10		
			7.10	0.00	0.00	0.00
			88.45	13.11	13.11	88.10

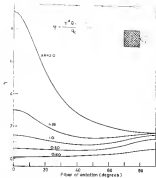


FIG. 3 MAXIMUM DEFLECTION OF SIMPLY SUPPORTED LAMINATED PLATE VS. FIBER ORIENTATION



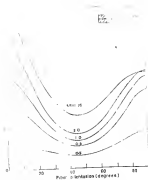


Fig. 10. Variation of isochronal stresses with fiber separation.

67

Figure 1  
 Stress vs. Fiber Orientation

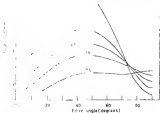


FIG. 1. VARIATION OF SHEAR STRESS VS. FIBER ORIENTATION

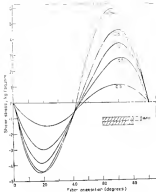


FIG. 3.4. VARIATION OF SHEAR STRESS WITH FIBER ORIENTATION

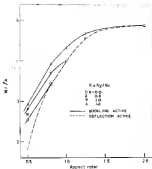


FIG. 3.5 VARIATION OF OPTIMUM WEIGHT WITH ASPECT RATIO

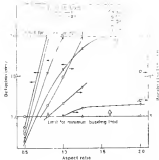


FIG. 16. VARIATION OF DEFLECTION AND BUCKLING LOAD WITH ASPECT RATIO FOR OPTIMUM VIBRANT SYSTEM

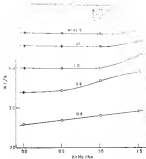


FIG. 10. VARIATION OF OPTIMIZATION WITH DEPTH WITH SPATIAL LOADING RATIO

## CHAPTER 4

### OPTIMUM WEIGHT DESIGN OF THE 4-2254-207 AIRCRAFT

#### COMPOSITE PLATES

##### 4.1 INTRODUCTION

In the previous chapters, a laminated plate with orthotropic laminae is considered for optimum weight design. This orthotropy is achieved by assigning an equal number of fibers at positive and negative orientations with respect to the structural axis, in a matrix or a ply. In this chapter, another class of laminated composite plates is considered, namely, the antisymmetric angle-ply laminates. Coupling between in-plane stretching and twist exists in this case. Also, the coupling stiffness matrix elements  $B_{16}$  and  $B_{26}$  exist in this case. Shown, et. al. (2a) have shown that this coupling can be eliminated completely or partially by choosing the thickness ratios for plies suitably. It is well known that if this coupling is reduced or eliminated, the strength of laminates improves.

Again, an attempt is made to obtain a minimum weight design for antisymmetric angle-ply laminates subjected to in-plane compressive and transverse loadings. The term antisymmetric is used in the sense that laminate thickness distributions with positive and negative fiber

orientation  $\alpha_i$  depend on a pair distance  $l_{ij}$  and structural data. The analysis is very complex and can be applied to any type of arrangement.

The following studies are conducted on each planet

- (1) Minimum weight design of nonsynchronous rigid-body laminae with variable thickness of  $0.01 \text{ m}$ . The fiber orientations are pre-assigned.
- (2) Minimum weight design of synchronous rigid-plastic laminae meeting the thickness of plates and the corresponding fiber orientations as design variables.

### 4.2 PROBLEM IDENTIFICATION

For these problems the objective function is

$$\min \sum_{i=1}^{N/2} w_i, \quad \text{where, } i = \text{Total no. of plates.} \quad (77)$$

such that

$$-\pi/2 \leq \alpha_i \leq \pi/2, \quad i=1, N/2$$

$$t_i \leq t_1 \leq t_2, \quad i=1, N/2 \quad (78)$$

$$u \leq w,$$

$$x_2 \geq x_0,$$

$$\text{and} \quad \left( \frac{\sigma_{11}}{\sigma_{11}^0} \right)^2 + \left( \frac{\sigma_{22}}{\sigma_{22}^0} \right)^2 + \left( \frac{\sigma_{33}}{\sigma_{33}^0} \right)^2 + \left( \frac{\sigma_{12}}{\sigma_{12}^0} \right)^2 \leq 1$$





$$\text{Along } y = c, z,$$

$$\begin{aligned} \text{we } \quad v_f &= \tau_{22} u_f = (\tau_{12} + \tau_{21}) u_{10} + \tau_{22} u_{20} = 0 \\ v = 0 \quad \frac{\partial v}{\partial y} &= 0 \end{aligned} \quad (16)$$

The boundary, displacement conditions, satisfy the boundary conditions eqs. (a) and (b),

$$\begin{aligned} u &= \sum \sum A_{mn} \sin \frac{m\pi x}{a} \sin \frac{n\pi y}{b} \\ v &= \sum \sum B_{mn} \cos \frac{m\pi x}{a} \sin \frac{n\pi y}{b} \\ w &= \sum \sum C_{mn} \sin \frac{m\pi x}{a} \sin \frac{n\pi y}{b} \end{aligned} \quad (17)$$

Substituting Eq. (17) in Eqs. (1) and (6) we get Eq. (11) as an expression for the buckling load, where  $\tau_{21}$  is defined by Eq. (11), except  $\tau_{12}$  and  $\tau_{22}$  which are as follows :

$$\begin{aligned} \tau_{12} &= \left\{ 2\mu_{12} a^2 \pi^2 + 2\mu_{22} a^2 \pi^2 (a/b)^2 \right\} a u(a/b) \\ \tau_{22} &= \left\{ 2\mu_{12} a^2 + 2\mu_{22} a^2 + 2(a/b)^2 \right\} a \pi^2 \end{aligned} \quad (18)$$

Deflection under transverse loading is given by Eq. (11), in which,  $\tau_{12}$  and  $\tau_{22}$  are defined in Eq. (18).



## 5.4. DESIGN AND ANALYSIS

### 5.4.1. Design

Minimum weight optimization is an iterative limited composite plate is divided into  $n$  rectangular number of slices and aspect ratio for length/width composite whose material properties are  $E$  and  $\nu$  is section (2.4.1).

Maximize subject to the constraints for the following set of constraints :

Longitudinal tensile strength = 160,000 kg/sq.cm.  
 Transverse tensile strength = 8.45 kg/sq. cm.  
 Longitudinal compressive strength = 18.13 kg/sq.cm.  
 Transverse compressive strength = 18.11 kg/sq.cm.  
 Shear strength = 11.05 kg/sq.cm.  
 Modulus under compression = 0.005 kg/sq.cm.  
 Upper limit on maximum deflection = 0.05 cm  
 minimum bending load is = 1000 kg/cm.  
 minimum thickness of each ply = 0.101 mm.  
 maximum thickness of each ply = 2.5 mm

Table 5.1 shows that for a four ply unsymmetric laminate a thickness ratio of 0.416 is attained at optimum design. The fiber orientation of approximately  $15^\circ$  results in minimum weight design for an aspect ratio of 0.5 and  $\nu = 0.3$ .

Fig. 4.1 illustrates the variation of optimum number of piles at fixed aspect ratio of 1.0 and fixed load for various values of axial loading ratio. The optimum value of  $N$  and  $W_{opt}$  is shown in Fig. 4.2.

Tables 4.3 and 4.4 show the optimum pile arrangement for different pre-designed filter orientations. The results showed that the optimum design is achieved by the pile of piles with optimum diameter and thickness. All other piles resulted higher weight of pile.

Fig. 4.3 presents the variation of pile thickness ratio with increasing values of aspect ratio. The thickness ratio of square pile type is 1.0 for optimum value. It appears that, if the constraints on pile thickness is removed, for every pile, it is possible, if the weight of pile is very high. The other pile thickness ratios are very close to unity and hence almost constant.

As shown results are for a pre-designed filter orientation. Table 4.5 shows the variation of the optimum filter orientation and corresponding thickness with aspect ratio and biaxial loading ratio. The optimum weight increases with increasing aspect ratio and biaxial loading ratio. The thickness ratio decreases with increasing biaxial loading ratio, however, the

design of the sandwich plate and the corresponding critical distance  $l_c$  is reported in Table 1. The critical distance  $l_c$  is the distance from the loading point to the free edge of the plate. It is seen that the critical distance  $l_c$  is larger for a plate with increasing  $\rho$  and  $\mu$ . The critical distance  $l_c$  is also larger for a plate with increasing  $\rho$  and  $\mu$ . The critical distance  $l_c$  is also larger for a plate with increasing  $\rho$  and  $\mu$ . The critical distance  $l_c$  is also larger for a plate with increasing  $\rho$  and  $\mu$ .

Table 1 also presents the critical distance  $l_c$  for the thickness and the corresponding linear distance  $l_c$  for the increasing number of plies. The linear distance  $l_c$  of plies near the mid-ply is reported in Table 1. The corresponding thickness  $h$  corresponds to the linear assigned value.

### 3.4.3. Optimal Design

The optimal thickness rule for the sandwich weight is 4.404 for the four ply sandwiched laminated plate. This thickness rule is identical with the one reported by Shari, et al. (18) to remove coupling effects. The thickness  $h$  rule for the sandwich sandwiched core, see also the sandwich rule of reference (18), where  $h$  is the thickness of the

$$h_2 = (h_1 - 1) \pm \sqrt{(h_1^2 - 1)} \quad (22)$$



analysis, results of the present analysis are compared with the experimental results in section 4.4.

### 4.3. CONCLUSIONS

The following conclusions are drawn from the results obtained:

- (1) A satisfactory solution, characterized by a low in the specified range, has been obtained by a proposed filter characteristic for the filter, Fig. 2.1.1.
- (2) When the thickness and the filter value are taken as the design variables, it appears that in addition to the thickness there is a function, as optimum values, and value of filter characteristic also appears as optimum.
- (3) The general conclusions which are drawn from the results are also applicable here as discussed in section 4.4.2.





$$v_{\text{eff}}/v_{\text{th}} = \frac{v_{\text{eff}}}{v_{\text{th}}}$$

Effective fiber orientation = 1.10

Fiber content ratio	Fiber Orientation										Effective Fiber Ratio
	$v_1$	$v_2$	$v_3$	$v_4$	$v_5$	$v_6$	$v_7$	$v_8$	$v_9$	$v_{10}$	
1	0.1000	1.0000	0.0000								0.1000
2	0.1000	0.9000	0.0000								0.1000
3	0.1000	0.8000	0.0000								0.1000
4	0.1000	0.7000	0.0000								0.1000
5	0.1000	0.6000	0.0000								0.1000
6	0.1000	0.5000	0.0000								0.1000
7	0.1000	0.4000	0.0000								0.1000
8	0.1000	0.3000	0.0000								0.1000
9	0.1000	0.2000	0.0000								0.1000
10	0.1000	0.1000	0.0000								0.1000

1.10

[illegible]



$$\text{Altitude of the sun on 21 March} = +10^\circ$$
[illegible]



Designation	M <sub>1</sub> kg/cm <sup>2</sup>	Applied stress (kg/cm <sup>2</sup> )		σ <sub>1</sub> kg/cm <sup>2</sup>	σ <sub>2</sub> kg/cm <sup>2</sup>	Deformation mm/mm	Notched control specimen	σ <sub>1</sub> kg/cm <sup>2</sup>	σ <sub>2</sub> kg/cm <sup>2</sup>
		σ <sub>1</sub>	σ <sub>2</sub>						
A-1	0.0	0.00	0.000	0.00	-0.000	0.00	unloading	0.0	0.00
	0.5	0.500	0.7500	7.50	-0.500	0.00	downloading	0.750	0.00
	1.0	0.500	0.5000	5.00	-0.500	0.00	unloading	0.500	0.00
A-2	0.0	0.000	1.1000	11.00	-0.000	0.00	distraction	0.00	0.00
	0.5	0.500	1.1000	11.00	-0.500	0.00	unloading	0.500	0.00
	1.0	0.500	1.1000	11.00	-0.500	0.00	distraction	0.500	0.00
A-3	0.0	0.000	1.1000	11.00	-0.000	0.00	distraction	0.00	0.00
	0.5	0.500	1.1000	11.00	-0.500	0.00	distraction	0.500	0.00
	1.0	0.500	1.1000	11.00	-0.500	0.00	distraction	0.500	0.00

$$\text{equivalent ratio} = 1.0$$

$$x = b_1/b_0 = 0.9$$

Total thickness of section	Typical case, no ducts						Typical case with ducts
	$b_1/b_0$	$b_2/b_0$	$b_3/b_0$	$b_4/b_0$	$b_5/b_0$	$b_6/b_0$	
4	0.99997	0.99998					5.01
	-0.00010	-0.00002					
6	0.99991	0.99995	0.99990				1.96
	-0.00008	-0.00003	-0.00007				
11	0.99984	0.99993	0.99991	0.99991			4.03
	-0.00016	-0.00006	-0.00009	-0.00009			
19	0.99988	0.99997	0.99998	0.99997	0.99999		6.09
	-0.00012	-0.00003	-0.00002	-0.00003	-0.00001		
1.0	0.99974	0.99995	0.99996	0.99997	0.99999	0.99999	14.09
	-0.00026	-0.00005	-0.00004	-0.00003	-0.00001	-0.00001	

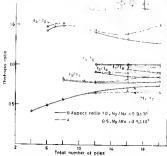


FIG. 4.1 THICKNESS RATIO VS TOTAL NUMBER OF PILES

## CHAPTER 1

### INTRODUCTION

The key to the structural design of composite structures is the proper use of the optimization techniques for more efficient utilization of the material, at whatever circumstances. Each contains the potential use of all the design possibilities provided by composites is the intrinsic complication involved at macro-mechanical and micro-mechanical levels of the analysis of such materials. However, lot of theoretical structures have been used and the usage of optimization techniques is gaining momentum.

In order to comprehend and appreciate the varied role which the application of optimization techniques can play, it is worthwhile to point out here, that a reduction by one-tenth of a millimeter of thickness, for a plate of size 100 cm x 100 cm, results in material cost-savings of approximately, 1-2 %. For carbon/epoxy composite cost projection, at present, this does not include the operational cost-savings, which will be tremendous in the case of aerospace applications.

In this thesis, the optimization studies have been carried out, incorporating a set of design variables to achieve more flexibility in the design, to get a



minimization design of 1-dimensional minimax filter. Particular cases of particular sets of special, orthogonally invariant and invariant, and single-pole invariant sets are considered. Maximizing filter design is obtained by using the maximization and minimization of the error function and analysis to analytical form with its some numerical, techniques, which, besides being appropriate in terms of time and time consuming, strongly supported by many techniques which are available to obtain from numerical data and used throughout the study.

In the following sections, the conditions drawn at the end of each chapter is presented.

The constrained optimization problem is transformed into a series of unconstrained optimization problems, using interior penalty function approach. It should be noted that the filter error surface (single variables) enter the transformed function through the constraints. Objective function does not contain the filter coefficients as variables. For higher values of the penalty parameter, none of the constraints become active. Transformed objective function has the minimum away from the constraint surfaces) or in other words, behavior, and side constraint contribute almost equally to the objective function. This results in the filter coefficients achieving an optimal value, with every constraint contributing almost equally

to it, before numerical optimization, after the design parameter is fixed to a fixed value, the entire relationship constraints concerning to the objective function. Due to this, the initial derivative of the stress field, stress gradients are low compared with case, initially, and then reach the optimum value. This does not affect the optimal weight appreciably.

The total computational time taken by the algorithm is dependent on the design problem, the fixed design value and other factors. In view of this, any comparison of total computational time is not attempted. But stress and deflection analysis takes about 0.13 second and if analytical derivatives are calculated, an additional time of about 0.07 second is added. For calculating the numerical derivatives, the algorithm takes about 0.88 second. Hence, analytical derivative calculation results in less CPU (Central Processing Unit) time.

The following general conclusions can be drawn from the study conducted :

- (1) Maximum buckling load is obtained when the total thickness of the plate assumes the optimum fiber orientation for a given aspect ratio and classical loading pattern.

- (2) The designer of the composite will not need any volume manufacturing constraints, i. e. to place near the mid-plane, etc. criteria.
- (3) The weight per unit area of the plate decreases with increasing aspect ratio, i.e., it tends to approach an asymptotic value with aspect ratio.
- (4) Designs never become negative in optimum when the low deflection regime set on the various designs. These constraints can be relaxed to improve the efficiency of the designs.
- (5) The optimum for an orthotropic high-ply laminate is obtained when the ply stack-ups take particular values.

#### SCOPE OF THE PRESENT WORK

The logical extension of the present work can be stated as follows :

- (1) A general orthotropic laminated ply can be considered with various boundary conditions.
- (2) Volume fraction of the fibres and the matrix of each ply can be incorporated as a design variable to get an optimum weight structure.
- (3) Optimization of hybrid laminates.



- (17) Talmon, G., "Methods and Codes for the design of optimal design of flexible and composite structures subject to strength and buckling constraints", Proc. symposium, structural dynamics and related conference, San Diego, California, March 21-22, 1977.
- (18) Abu, F.A., "Computer programs (ALCOFF) for optimization of composite structures for minimum weight design", U.S. Air Force Dynamic Laboratory, Tech. Report AFRL-DR-76-148, 1977, pp. 54.
- (19) McKeown, J.J., "Optimal composite structures by dedication variable programming", Computer Methods in Applied Mechanics and Engineering, Vol. 11, 1977, pp. 155-179.
- (20) McKeown, J.J., "A new approach to the optimization multi layered composite structures", Proc. International journal of astronautical Sciences symposium 1979, Lisbon, Portugal, Sept. 10-14, 1979, Vol. 1.
- (21) McKeown, J.J., "A quasi-linear programming algorithm for optimizing fiber reinforced structures of fixed stiffness", Computer Methods in applied Mechanics and Engineering, Vol. 6, 1976, pp. 123-134.

- (12) Chan, C.C., An, L.H. and Sun, C.T., "Optimization of stacking the ply sequence and laminate composition", *Adv. Mater.*, Vol. 11, No. 1, 1971, pp. 1111 - 1121.
- (13) Schmit, G.G., C.A. and Farghal, S., "Optimal design of laminated fiber composite plates", *Composites*, Vol. 8 for Particular, *Methods in Engineering*, Vol. 11, No. 4, 1977, pp. 423-443.
- (14) Hagedorn, P., "Optimization and elastic stability strength of fiber reinforced composite structures - concepts, practice and optimization", Proceedings of symposium, Syntex, Society of American Science, Japan, 1974, pp. 369-409.
- (15) Hagedorn, P., "Optimum design of laminated plates under axial compression", *Adv. Mater.*, Vol. 17, 1979, pp. 1217-1218.
- (16) Sharda, S., Dwyer, F.G.A. and Murthy P.L., "Some comments on coupling of angle ply laminates", *J. structural mechanics*, Vol. 7, 1979, pp. 413-423.
- (17) Swamy, L.N., and Krenk, S.A., Ed. "Composite materials" Vol. 2, Gordon and Breach, 1974.
- (18) Dwyer, F.G.A., and Chao, S.A., "Programming methods in structural design" Affiliated Services Press Private Limited, Delhi, 1980.

- (18) Wilson, R.H., "Applied as an anti-aircraft missile",  
Spring, 1944, 1945.
- (19) Wilson, R.H., "The design of a missile, aircraft  
engine, and the aircraft engine",  
New York, 1945.

# APPENDIX 1

The gradients of the modified moments are divided in two following terms:

$$\frac{\partial \mu_{k+1}^{(n)}}{\partial \alpha_k} = \frac{\partial}{\partial \alpha_k} \left( \frac{-\partial \mu_k^{(n)}}{\partial \alpha_k} (x_k - x_{k-1}) \right) + \frac{\partial \mu_k^{(n)}}{\partial \alpha_k} \left( -\frac{\partial x_k}{\partial \alpha_k} + \frac{\partial x_{k-1}}{\partial \alpha_k} \right)$$

$$\begin{aligned} \frac{\partial \mu_{k+1}^{(n)}}{\partial \alpha_k} &= \frac{\partial}{\partial \alpha_k} \left( \frac{1}{3} - \frac{\partial \mu_k^{(n)}}{\partial \alpha_k} (x_k^2 - x_{k-1}^2) \right) \\ &+ \left( \mu_k^{(n)} + x_k \frac{\partial x_k}{\partial \alpha_k} - x_{k-1} \frac{\partial x_{k-1}}{\partial \alpha_k} \right) \end{aligned}$$

$$\begin{aligned} \frac{\partial \mu_{k+1}^{(n)}}{\partial \alpha_k} &= \frac{\partial}{\partial \alpha_k} \left( \frac{1}{3} - \frac{\partial \mu_k^{(n)}}{\partial \alpha_k} (x_k^2 - x_{k-1}^2) \right) \\ &+ \mu_k^{(n)} \left( \mu_k^{(n)} - \frac{\partial x_k}{\partial \alpha_k} + \frac{\partial x_{k-1}}{\partial \alpha_k} \right) \end{aligned}$$

where

$$\begin{aligned} x_1 &= x_0 && \text{for } \text{mod}_2(N)/2 \\ &&& \text{mod}_2(1) \end{aligned}$$

$$\begin{aligned} x_k &= t_k && \text{for } \text{mod}^2(2k), \quad 1 \leq k \leq N/2 \\ &&& \text{mod}^2(1), \quad k \geq 1 \end{aligned}$$

and

$$\frac{\partial \mu_{k+1}^{(n)}}{\partial \alpha_k} = 0 \quad \text{for } k \geq N$$



and

$$\frac{\partial \tilde{g}_{11}^{(1)}(x)}{\partial x^1} = -\alpha \tilde{v}_2 \sin(2\theta(x)) - \alpha \tilde{v}_2 \sin(2\theta(x))$$

$$\frac{\partial \tilde{g}_{12}^{(1)}(x)}{\partial x^1} = +\alpha \tilde{v}_2 \sin(2\theta(x))$$

$$\frac{\partial \tilde{g}_{22}^{(1)}(x)}{\partial x^1} = 2\alpha \tilde{v}_2 \sin(2\theta(x)) = +\alpha \tilde{v}_2 \sin(4\theta(x))$$

$$\frac{\partial \tilde{g}_{11}^{(1)}(x)}{\partial x^2} = \alpha \tilde{v}_2 \cos(2\theta(x)) + \alpha \tilde{v}_2 \cos(2\theta(x))$$

$$\frac{\partial \tilde{g}_{12}^{(1)}(x)}{\partial x^2} = \alpha \tilde{v}_2 \cos(2\theta(x)) - \alpha \tilde{v}_2 \cos(2\theta(x))$$

$$\frac{\partial \tilde{g}_{22}^{(1)}(x)}{\partial x^2} = 4\alpha \tilde{v}_2 \sin(4\theta(x))$$

$$\partial_{\mu} \tilde{g}_{\mu\nu} = 0$$

where

$$\tilde{v}_2 = \frac{G_{11} - G_{22}}{2}$$

$$\tilde{v}_2 = \frac{G_{11} + G_{22} - G_{12} - G_{21}}{2}$$

and

$$\frac{\partial \tilde{g}_{\mu\nu}}{\partial x^{\mu}} = \frac{1}{2} \partial_{\mu} \tilde{g}_{\mu\nu} = 0$$

and  $\tilde{g}_{\mu\nu} \neq 0$

$$= \frac{1}{2} \partial_{\mu} \tilde{g}_{\mu\nu} \quad \text{if } \tilde{g}_{\mu\nu} \neq 0$$

$$= 0 \quad \text{if } \tilde{g}_{\mu\nu} = 0$$

$$= \alpha \tilde{v}_2 = 0$$

where

$$\begin{aligned}
 a_0 &= -\frac{1}{2} \sum_{k=1}^{\infty} \frac{1}{k} \quad \text{and} \quad a_1 = 0 \\
 a &= \frac{1}{2} \sum_{k=1}^{\infty} \frac{1}{k} \quad \text{and} \quad a_2 = \frac{1}{2} \sum_{k=1}^{\infty} \frac{1}{k} \quad \text{and} \quad a_3 = 0 \\
 a &= \frac{1}{2} \sum_{k=1}^{\infty} \frac{1}{k} \quad \text{and} \quad a_4 = \frac{1}{2} \sum_{k=1}^{\infty} \frac{1}{k} \quad \text{and} \quad a_5 = 0 \\
 a &= \frac{1}{2} \sum_{k=1}^{\infty} \frac{1}{k} \quad \text{and} \quad a_6 = \frac{1}{2} \sum_{k=1}^{\infty} \frac{1}{k} \quad \text{and} \quad a_7 = 0 \\
 a &= 0 \quad \text{and} \quad a_8 = 0
 \end{aligned}$$

(See Fig. 3.1)